Simultaneous Input-State Estimation with Direct Feedthrough Based on a Unifying MMSE Framework with Experimental Validation

Xi Liu[a], Yang Wang[a,b,*] and Erik I. Verriest[b]

[a] *School of Civil and Environmental Engineering, Georgia Institute of Technology, Atlanta, GA, USA*
[b] *School of Electrical and Computer Engineering, Georgia Institute of Technology, Atlanta, GA, USA*
* *yang.wang@ce.gatech.edu*

Abstract: This paper addresses the simultaneous input-state estimation problem for discrete-time linear stochastic systems with unknown input. A unifying minimum-mean-square-error (MMSE) estimation framework is presented for a comprehensive characterization and direct comparison among a few popular input estimation approaches. In this work, the dynamical model of the input is assumed to be unknown and the input is treated as a random variable at each time step. To account for the unknown input dynamics, we propose an input estimator that adopts a white Gaussian input model with a finite covariance, short-named as the FIC (finite input covariance) estimator. Theoretical formulation of the FIC estimator is first compared with two other estimators, one using a Gaussian random walk input model combined with augmented Kalman filter (AKF) and another one using a deterministic input model with weighted least squares (WLS) estimation. Based on the unifying MMSE framework presented in this paper, it is proved that when the input covariance of the FIC estimator approaches infinity and the feedthrough matrix has full-column rank, the estimator is equivalent to the well-known WLS estimator.

The FIC estimator is validated and compared with the AKF and WLS estimator using simulated measurements from 2-story shear structure and experimental measurements from a full-scale concrete frame. The 2-story shear structure is excited by two different types of input and the corresponding acceleration responses are used to compare estimator performance. With only acceleration measurements, the FIC estimator eliminates a low-frequency drift error in the estimated input and states with a tight estimation confidence interval. Detailed discussion on the effect of estimator covariances on input estimation is also provided. *A priori* knowledge of the statistical property of the unknown input can provide insights in the tuning of FIC estimator covariances. In addition, field acceleration measurements from a full-scale concrete frame under shaker excitation are used to compare the estimation results and validate the proposed FIC estimator. The FIC estimator is shown to provide better estimates with tighter estimation confidence interval in comparison to the AKF and WLS estimators.

Keywords: input estimation; minimum-mean-square-error estimator; linear stochastic system; modal analysis; dynamic testing

1. Introduction

State estimation of dynamical systems subject to unknown inputs plays a vital role in many engineering applications, such as fault detection, geophysical applications, communication systems, target tracking and navigations [1, 2]. For example, in some structural engineering applications, it is often expensive or not feasible to measure the input/excitation directly. Instead, an explicit estimate of the unknown input can be performed. The simultaneous input-state estimation problem can be grouped into two major categories based on the system model: (1) when the output y does not contain the unknown input u (i.e. $D = 0$, without direct feedthrough); (2) when the output contains all the unknown input (i.e. $D \neq 0$, with direct feedthrough).

Among early contributions to account for unknown input or bias, Friedland proposed a two-stage Kalman filter to estimate a constant bias by augmenting the state vector with the unknown bias vector [3]. Verriest generalized the constant bias assumption to time-varying bias/input signals with random initial conditions as well as for systems with delays [4]. This generalization required a state space model of the unknown input. For problems without state space model of the input, Kitanidis proposed a recursive state estimator by minimizing the trace of the state estimation error covariance for systems without direct feedthrough [1]. This approach provided an optimal state estimation in the sense of minimum mean square error (MMSE), but did not explicitly estimate the unknown input. Darouach *et al.* extended Kitanidis's estimator to systems with direct feedthrough for state estimation under unknown inputs [5]. To obtain an explicit estimation of the unknown input, Gillijns *et al.* combined the state estimation from Kitanidis with a weighted least squares (WLS) estimator of the unknown input for systems with direct feedthrough [6]. Lourens *et al.* extends the WLS filter for reduced-order models especially when the number of sensors exceeds the model order [7]. Maes *et al.* extended the WLS filter to consider correlated process and measurement noise [8] and validated the algorithm using field measurements of a footbridge for impact force identification [9]. It should be noted that when WLS is used in the aforementioned algorithms to estimate the unknown input, the input is treated as deterministic at each time step without utilizing any estimation results from prior time steps. Another approach is to treat the unknown input as a random variable and augmenting it to the state vector based on a Gaussian random walk model, proposed by Lourens *et al.* for force identification [10]. In this approach, the covariance of the unknown input

needs to be tuned properly based on an L-curve method. It was also reported that when using acceleration measurements alone, a low-frequency drift occurs in both the estimated input and state and the augmented system suffers from un-observability issue [10]. To improve the estimator performance and eliminate the drift error, Azam *et al.* proposed a dual Kalman filter by switching the measurement update of the unknown input and time update of state, thus separating input and state estimation into two stages [11]. This approach has the underlying assumption that the unknown input and state are uncorrelated. Although it is shown to be able to reduce drift error, similar as the augmented Kalman filter, it also required a properly tuned covariance and the estimator performance is quite sensitive to the parameter [12]. Other approaches to reduce the drift error include the use of post-processing high-pass filtering [9], fictitious displacement measurements [13], and an online high-pass filter [14].

Recently, to overcome the drift error, researchers have started to incorporate prior information of the unknown input in the estimation process. Valikhani, *et al.* [15] proposed a Bayesian framework to include prior distribution of the unknown input for systems with and without direct feedthrough of the input. The input covariance matrix is tuned offline through the L-curve method, using the entire measurement time histories. Similarly, Sedehi, *et al.* [16] proposed a sequential Bayesian estimation framework by assuming that the input covariance is obtained from the input estimation error covariance at the preceding time step; the noise covariance matrices are updated in real time using asymptotic approximations. Besides assuming prior distribution of the unknown input, dynamic models of the input can also be combined in the estimation process [17-20]. For example, Nayek, *et al.* [17] proposed to use a Gaussian process latent force model for the unknown input; similar to the L-curve method, offline calibration of the input hyperparameters need to be first tuned using the entire measurement time histories before online estimation can be executed.

In input-state estimation, modeling accuracy of the underlining dynamical system can affect the estimation accuracy. Some researchers proposed to estimate system parameters along with input and state estimation. Sun, *et al*. [21] proposed an iterative Bayesian inference-based regularization approach for input estimation where drift error can be removed. This offline method updates both structural parameters and unknown input forces iteratively via regularized optimization process. In addition, the unknown force time history and the regularization parameters can be updated iteratively to estimate traffic-induced nodal excitations through least squares [22]. In addition to the offline least squares approaches, recursive estimators are also proposed to estimate input, state and system parameters

simultaneously using heterogeneous sensor measurements. Examples include extended Kalman filter combined with parametric model reduction for linear structures [23], unscented Kalman filter [24, 25] and extended Kalman filter [26, 27] for nonlinear structures. When a linear time invariant model is adopted for a structure, vibration modal properties (such as natural frequencies, mode shapes, and damping ratios) extracted from experimental measurements can be used to first evaluate the behavioral similarities between an as-built structure and the corresponding structural model. If significant discrepancies are found, frequency-domain approaches can be used to update certain model parameters based on vibration modal properties extracted from experimental data, a process known as finite element model updating [28-32].

When monitoring the structural response of civil structures, acceleration measurements are extensively used and additional displacement measurement may not be available in each field test scenario. Therefore, the low-frequency drift error when displacement sensors are not available needs to be further studied to guarantee a good estimate of both the unknown input and state, especially for long-term structural monitoring. In this paper, we propose an online input-state estimator by assuming the prior distribution of the unknown input as white Gaussian. An explicit estimate of the input can be derived so that the drift error can be eliminated when only acceleration measurements are available. Although it is common to treat the unknown input as zero-mean white Gaussian noise when using output-only data for modal identification [33] and state estimation [34], an explicit estimation of both input and state needs to be derived under the white Gaussian input assumption. Under the white Gaussian input assumption, the un-observability issue presented in early research studies can be resolved. In comparison to the method proposed in [15], three sets of estimator equations are derived and simplified to account for unknown input with small, large and infinite covariances, respectively.

In addition, this paper uses an MMSE framework to systematically compare the proposed white noise estimator with finite input covariance (FIC) with the random walk estimator based on augmented Kalman filter (AKF) proposed in [10] and the WLS estimator proposed in [6]. Underlying connections between the three estimators are revealed through the unifying MMSE framework. Because all of these input-state estimators can be incorporated into the same unifying MMSE framework, theoretical relationship among these three estimators are derived in this paper to provide unifying and comparative insights. Note that for all three estimators, the dynamics of the input is assumed to be unknown, i.e. no state space model of the input is available as prior knowledge. In this case, the AKF

assumes a random walk model of the unknown input; the FIC estimator treats the input as white Gaussian noise with a predefined input covariance Σ_u; and the WLS estimator is proved here to be equivalent as the FIC estimator when the input covariance of the FIC estimator approaches infinity, i.e. $\Sigma_u = \Sigma_\infty$. Numerical examples of white noise input and sinusoidal input are provided to validate the proposed FIC estimator in comparison to AKF and WLS estimator. Detailed discussion on the choice of estimator covariances is also included by utilizing the statistical property of the input as prior knowledge. Furthermore, experimental validation based on a full-scale concrete frame using acceleration measurements is presented. Model order of the full-scale structure is reduced based on modal decomposition. Effect of sensor instrumentation on input estimation using the reduced-order model is also investigated.

The rest of the paper is organized as follows. Section 2 introduces the problem of simultaneous input-state estimation with assumptions made in the paper and lemmas used in the derivations in the following section. In Section 3, we first present the basic unifying MMSE framework by augmenting the unknown input to the state vector in measurement update but keeping the estimation of input and state separate. Next, time update of input and state is derived based on the random walk input model and the white noise input model. Finally, proof is provided to show that when Σ_u of the FIC estimator approaches infinity and the feedthrough matrix D has full-column rank, the WLS estimator can be obtained. Section 4 provides numerical examples of a 2-story shear structure excited by white noise input and sinusoidal input, respectively. Given acceleration measurements, comparison of the FIC, AKF and WLS estimators is provided. Section 0 validates the proposed FIC estimator and compares all estimator performance on a full-scale concrete frame structure using both simulated and experimental acceleration measurements.

2. Problem formulation

Consider the following discrete-time stochastic linear system with direct feedthrough of input:

$$x_{k+1} = Ax_k + Bu_k + w_k \tag{1}$$

$$y_k = Cx_k + Du_k + v_k \tag{2}$$

where $x_k \in \mathbb{R}^n$ is the state at time step k, $u_k \in \mathbb{R}^{n_u}$ is the unknown input, $w_k \in \mathbb{R}^n$ is the process noise or disturbance, $y_k \in \mathbb{R}^m$ is the measurement output, and $v_k \in \mathbb{R}^m$ is the measurement noise. The unknown input u_k is

assumed to be a random variable at each time step with unknown dynamics. To account for the unknown dynamics, the first approach, proposed in [10], assumes a random walk model of the unknown input with white Gaussian process noise $\xi_k \sim \mathcal{N}(0, \Sigma_{\xi_k})$, i.e. $u_{k+1} = u_k + \xi_k$, where ξ_k is independent from x_0, u_l, v_l and w_l for all k and l. The covariance of ξ_k is assumed to be time invariant, i.e. $\Sigma_{\xi_k} = \Sigma_\xi$. The second approach assumes the input has white Gaussian distribution with a predefined finite input covariance Σ_u to utilize any prior knowledge related to the input. The third approach extends the finite input covariance to be infinite, i.e. $\Sigma_u = \Sigma_\infty$, when assuming the input is highly uncertain.

The additional assumptions are: (1) the system is observable, i.e. (A, C) is observable; as a result, the rank of the observability matrix $\mathcal{O} = [C^T \quad (CA)^T \quad \cdots \quad (CA^{n-1})^T]^T$ equals the number of states n; (2) $v_k \sim \mathcal{N}(0, \Sigma_v)$ and $w_k \sim \mathcal{N}(0, \Sigma_w)$ are white Gaussian noise such that Σ_v and Σ_w are diagonal matrices and $\Sigma_v \succ 0$ and $\Sigma_w \succcurlyeq 0$; (3) v_k and w_l are independent for all k and l; (4) initial state is random $x_0 \sim \mathcal{N}(\mu_0, \Sigma_0)$ and independent from v_k and w_l for all k and l; (5) unknown input u_k^{seq} is Gaussian and independent from x_0, v_l and w_l for all k and l.

The following notations are used here: the minimum-mean-square-error (MMSE) estimate of x_k given cumulative sequential measurements $y_l^{\text{seq}} \triangleq [y_0^T \quad y_1^T \quad \cdots \quad y_l^T]^T$ is denoted as $\hat{x}_{k|l} \triangleq \mathbb{E}(x_k | y_l^{\text{seq}})$; the conditional covariance of x_k given y_l^{seq} is $\Sigma_{x_{k|l}} \triangleq \text{cov}(x_k | y_l^{\text{seq}})$; the MMSE of u_k is $\hat{u}_{k|l} \triangleq \mathbb{E}(u_k | y_l^{\text{seq}})$ with conditional covariance $\Sigma_{u_{k|l}} \triangleq \text{cov}(u_k | y_l^{\text{seq}})$. The conditional cross-covariance between the state and input is denoted as $\Sigma_{x_k u_{k|l}} \triangleq \text{cov}(x_k, u_k | y_l^{\text{seq}})$, and the conditional cross-covariance between the state-input vector $\begin{Bmatrix} x_k \\ u_k \end{Bmatrix}$ and measurement y_k is denoted as $\Sigma_{\begin{Bmatrix} x_k \\ u_k \end{Bmatrix} y_{k|l}} \triangleq \text{cov}\left(\begin{Bmatrix} x_k \\ u_k \end{Bmatrix}, y_k \middle| y_l^{\text{seq}}\right)$.

Four lemmas are provided here to assist the derivation in Section 3. Since the first three lemmas are standard, they are provided without proof.

Lemma 1 (matrix push through identity) Let $A \in \mathbb{R}^{m \times n}$, $B \in \mathbb{R}^{n \times m}$, I_m is the identity matrix with dimension $m \times m$ and both $(I_n + BA)$ and $(I_m + AB)$ are invertible. As a result,

$$A(I_n + BA)^{-1} = (I_m + AB)^{-1} A \tag{3}$$

Lemma 2 (Sherman-Morrison-Woodbury formula) Let $A \in \mathbb{R}^{m\times m}$, $B \in \mathbb{R}^{m\times n}$, $C \in \mathbb{R}^{n\times n}$, $D \in \mathbb{R}^{n\times m}$. If A, C, $A + BCD$, and $C^{-1} + DA^{-1}B$ are nonsingular,

$$(A + BCD)^{-1} = A^{-1} - A^{-1}B(C^{-1} + DA^{-1}B)^{-1}DA^{-1} \tag{4a}$$

$$= A^{-1}(I_m - B(C^{-1} + DA^{-1}B)^{-1}DA^{-1}) \tag{4b}$$

Lemma 3 Suppose $x \in \mathbb{R}^n$ and $v \in \mathbb{R}^m$ are independent random vectors. We would like to estimate x based on a linear measurement $y = Ax + v$, where $A \in \mathbb{R}^{m\times n}$ is a constant matrix. As a result, we have $\mathbb{E}(y) = A\mathbb{E}(x) + \mathbb{E}(v)$, $\Sigma_{xy} = \Sigma_x A^T$ and $\Sigma_y = A\Sigma_x A^T + \Sigma_v$. If x, v are Gaussian, i.e. $x \sim \mathcal{N}(\mu_x, \Sigma_x)$, $v \sim \mathcal{N}(\mu_v, \Sigma_v)$, the MMSE estimate of x given y and the conditional estimation error covariance $\Sigma_{x|y}$ can be expressed as

$$\hat{x} = \mathbb{E}(x|y) = \mathbb{E}(x) + \Sigma_{xy}\Sigma_y^{-1}\big(y - \mathbb{E}(y)\big) \tag{5}$$

$$\Sigma_{x|y} \triangleq \mathrm{cov}(x|y) = \Sigma_x - \Sigma_{xy}\Sigma_y^{-1}\Sigma_{yx} \tag{6}$$

Note that x and y are also jointly Gaussian.

Lemma 4 For the system given by Eq. (1) and (2) with the assumptions made in Section 2, x_k, u_k, and y_k^{seq} are jointly Gaussian. In addition, given y_{k-1}^{seq}, vectors x_k, u_k, and y_k are individually and jointly Gaussian.

Proof. Based on (1) and (2), we can derive

$$x_k = A^k x_0 + H_{u_k} u_{k-1}^{\mathrm{seq}} + H_{w_k} w_{k-1}^{\mathrm{seq}} \tag{7}$$

$$y_k^{\mathrm{seq}} = \mathcal{O}_k x_0 + P_{u_k} u_k^{\mathrm{seq}} + P_{w_k} w_{k-1}^{\mathrm{seq}} + v_k^{\mathrm{seq}} \tag{8}$$

where $H_{u_k} = [A^{k-1}B \quad \cdots \quad AB \quad B]$, $H_{w_k} = [A^{k-1} \quad \cdots \quad A \quad I]$, $\mathcal{O}_k = \left[C^T \quad (CA)^T \quad \cdots \quad \left(CA^k\right)^T\right]^T$, $P_{u_k} = \begin{bmatrix} D & 0 & \cdots & 0 \\ CB & \ddots & \cdots & \vdots \\ \vdots & \ddots & D & 0 \\ CA^{k-1}B & \cdots & CB & D \end{bmatrix}$, $P_{w_k} = \begin{bmatrix} 0 & 0 & 0 \\ C & \ddots & \vdots \\ \vdots & \ddots & 0 \\ CA^{k-1} & \cdots & C \end{bmatrix}$.

Because x_0, u_k^{seq}, w_{k-1}^{seq} and v_k^{seq} are Gaussian and independent from each other, they are jointly Gaussian. Since x_k, u_k, and y_k^{seq} can be expressed as a linear transformation of x_0, u_k^{seq}, w_{k-1}^{seq} and v_k^{seq} with full row-rank as shown in Eq. (9), x_k, u_k, and y_k^{seq} are also jointly Gaussian.

$$\begin{Bmatrix} x_k \\ u_k \\ y_k^{\text{seq}} \end{Bmatrix} = \begin{bmatrix} A^k & \breve{H}_{u_k} & H_{w_k} & 0 \\ 0 & \check{I}_{n_u} & 0 & 0 \\ \mathcal{O}_k & P_{u_k} & P_{w_k} & I \end{bmatrix} \begin{Bmatrix} x_0 \\ u_k^{\text{seq}} \\ w_{k-1}^{\text{seq}} \\ v_k^{\text{seq}} \end{Bmatrix} \tag{9}$$

where $\breve{H}_{u_k} = [H_{u_k} \quad 0]$ and $\check{I}_{n_u} = [0 \quad I_{n_u}]$. Because conditional distributions of a Gaussian random vector are Gaussian, given y_{k-1}^{seq}, vectors x_k, u_k, and y_k are both individually and jointly Gaussian. ■

In the following section, a recursive MMSE estimator for simultaneous input-state estimation is derived assuming a random walk model, a white noise model with finite input covariance, and a white noise model with infinite input covariance, respectively.

3. Simultaneous input-state estimation

Given prior estimates of input and state at time step k, i.e. $\hat{x}_{k|k-1}$, $\Sigma_{x_{k|k-1}}$, $\hat{u}_{k|k-1}$, $\Sigma_{u_{k|k-1}}$ and $\Sigma_{x_k u_{k|k-1}}$, the state x_k and input u_k at time step k given measurements y_k^{seq} are simultaneously estimated based on a unifying MMSE framework.

3.1. Measurement update of input and state

Equation (2) can be rewritten in the following form by combining the state x_k and input u_k as a vector

$$y_k = [C \quad D] \begin{Bmatrix} x_k \\ u_k \end{Bmatrix} + v_k \tag{10}$$

Considering the independence of measurement noise v_k from past measurement sequence y_{k-1}^{seq}, Eq. (10) is conditioned on y_{k-1}^{seq} and the corresponding conditional expectation can be written as

$$\mathbb{E}\left(y_k \middle| y_{k-1}^{\text{seq}}\right) = [C \quad D]\mathbb{E}\left(\begin{Bmatrix} x_k \\ u_k \end{Bmatrix} \middle| y_{k-1}^{\text{seq}}\right) + \mathbb{E}(v_k) = C\hat{x}_{k|k-1} + D\hat{u}_{k|k-1} \tag{11}$$

Applying the affine transformation in Lemma 3 to Eq. (11), given y_{k-1}^{seq}, the conditional cross-covariance between $\begin{Bmatrix} x_k \\ u_k \end{Bmatrix}$ and y_k and the covariance of y_k are

$$\Sigma_{\begin{Bmatrix} x_k \\ u_k \end{Bmatrix} y_{k|k-1}} = \begin{bmatrix} \Sigma_{x_{k|k-1}} & \Sigma_{x_k u_{k|k-1}} \\ \Sigma_{u_k x_{k|k-1}} & \Sigma_{u_{k|k-1}} \end{bmatrix} \begin{bmatrix} C^T \\ D^T \end{bmatrix} \tag{12}$$

$$\Sigma_{y_{k|k-1}} = \begin{bmatrix} C & D \end{bmatrix} \begin{bmatrix} \Sigma_{x_{k|k-1}} & \Sigma_{x_k u_{k|k-1}} \\ \Sigma_{u_k x_{k|k-1}} & \Sigma_{u_{k|k-1}} \end{bmatrix} \begin{bmatrix} C^T \\ D^T \end{bmatrix} + \Sigma_v \tag{13}$$

Recall that measurement noise v_k is independent of x_k, u_k and y_{k-1}^{seq}, thus $\Sigma_{x_k v_{k|k-1}}$ and $\Sigma_{u_k v_{k|k-1}}$ are zero matrices. Expanding Eq. (12) and Eq. (13) gives the following expressions

$$\Sigma_{x_k y_{k|k-1}} = \Sigma_{x_{k|k-1}} C^T + \Sigma_{x_k u_{k|k-1}} D^T \tag{14}$$

$$\Sigma_{u_k y_{k|k-1}} = \Sigma_{u_{k|k-1}} D^T + \Sigma_{u_k x_{k|k-1}} C^T \tag{15}$$

$$\Sigma_{y_{k|k-1}} = C\Sigma_{x_{k|k-1}} C^T + D\Sigma_{u_{k|k-1}} D^T + \Sigma_v + D\Sigma_{u_k x_{k|k-1}} C^T + C\Sigma_{x_k u_{k|k-1}} D^T \tag{16}$$

Recall that given y_{k-1}^{seq}, vectors x_k, u_k, and y_k are jointly Gaussian from Lemma 4. Based on Lemma 3 the MMSE estimate of x_k, u_k given y_k and y_{k-1}^{seq} are shown in the following

$$\begin{aligned} \begin{Bmatrix} \hat{x}_{k|k} \\ \hat{u}_{k|k} \end{Bmatrix} &\triangleq \mathbb{E}\left(\begin{Bmatrix} x_k \\ u_k \end{Bmatrix} \middle| y_k^{\text{seq}} \right) = \mathbb{E}\left(\begin{Bmatrix} x_k \\ u_k \end{Bmatrix} \middle| y_{k-1}^{\text{seq}} \right) + \Sigma_{\begin{Bmatrix} x_k \\ u_k \end{Bmatrix} y_{k|k-1}} \Sigma_{y_{k|k-1}}^{-1} \left(y_k - \mathbb{E}\left(y_k \middle| y_{k-1}^{\text{seq}} \right) \right) \\ &= \begin{Bmatrix} \hat{x}_{k|k-1} \\ \hat{u}_{k|k-1} \end{Bmatrix} + \begin{bmatrix} \Sigma_{x_{k|k-1}} & \Sigma_{x_k u_{k|k-1}} \\ \Sigma_{u_k x_{k|k-1}} & \Sigma_{u_{k|k-1}} \end{bmatrix} \begin{bmatrix} C^T \\ D^T \end{bmatrix} \Sigma_{y_{k|k-1}}^{-1} \left(y_k - \mathbb{E}\left(y_k \middle| y_{k-1}^{\text{seq}} \right) \right) \end{aligned} \tag{17}$$

The last step holds by substituting $\Sigma_{\begin{Bmatrix} x_k \\ u_k \end{Bmatrix} y_{k|k-1}}$ from Eq. (12). Substitute Eq. (11), (14) ~ (16) into Eq. (17), we have

$$\begin{Bmatrix} \hat{x}_{k|k} \\ \hat{u}_{k|k} \end{Bmatrix} = \begin{Bmatrix} \hat{x}_{k|k-1} + L_{x_k}\left(y_k - C\hat{x}_{k|k-1} - D\hat{u}_{k|k-1} \right) \\ \hat{u}_{k|k-1} + L_{u_k}\left(y_k - C\hat{x}_{k|k-1} - D\hat{u}_{k|k-1} \right) \end{Bmatrix} \tag{18}$$

where the estimation gains are defined as

$$L_{x_k} \triangleq \Sigma_{x_k y_{k|k-1}} \Sigma_{y_{k|k-1}}^{-1} = \Sigma_{x_{k|k-1}} C^T \Sigma_{y_{k|k-1}}^{-1} + \Sigma_{x_k u_{k|k-1}} D^T \Sigma_{y_{k|k-1}}^{-1} \tag{19}$$

$$L_{u_k} \triangleq \Sigma_{u_k y_{k|k-1}} \Sigma_{y_{k|k-1}}^{-1} = \Sigma_{u_{k|k-1}} D^T \Sigma_{y_{k|k-1}}^{-1} + \Sigma_{u_k x_{k|k-1}} C^T \Sigma_{y_{k|k-1}}^{-1} \tag{20}$$

Note that $\Sigma_{x_k y_{k|k-1}}$ and $\Sigma_{u_k y_{k|k-1}}$ are given by Eq. (14) and (15). Based on Eq. (6) in Lemma 3, the conditional covariance given y_k^{seq} can be obtained as

$$\begin{aligned}\operatorname{cov}\left(\begin{Bmatrix}x_k\\u_k\end{Bmatrix}\middle|y_k^{\text{seq}}\right) &\triangleq \begin{bmatrix}\Sigma_{x_{k|k}} & \Sigma_{x_k u_{k|k}}\\ \Sigma_{u_k x_{k|k}} & \Sigma_{u_{k|k}}\end{bmatrix}\\ &= \begin{bmatrix}\Sigma_{x_{k|k-1}} & \Sigma_{x_k u_{k|k-1}}\\ \Sigma_{u_k x_{k|k-1}} & \Sigma_{u_{k|k-1}}\end{bmatrix} - \begin{bmatrix}\Sigma_{x_k y_{k|k-1}}\\ \Sigma_{u_k y_{k|k-1}}\end{bmatrix}\Sigma_{y_{k|k-1}}^{-1}\begin{bmatrix}\Sigma_{y_k x_{k|k-1}} & \Sigma_{y_k u_{k|k-1}}\end{bmatrix}\end{aligned} \tag{21}$$

Expand Eq. (21), simplify the equations with estimation gains and substitute $\Sigma_{x_k y_{k|k-1}}$ and $\Sigma_{u_k y_{k|k-1}}$ with Eq. (14) and (15)

$$\Sigma_{x_{k|k}} = \Sigma_{x_{k|k-1}} - \Sigma_{x_k y_{k|k-1}}\Sigma_{y_{k|k-1}}^{-1}\Sigma_{x_k y_{k|k-1}}^{T} = \Sigma_{x_{k|k-1}} - L_{x_k}\left(\Sigma_{x_{k|k-1}}C^T + \Sigma_{x_k u_{k|k-1}}D^T\right)^T \tag{22}$$

$$\Sigma_{u_{k|k}} = \Sigma_{u_{k|k-1}} - \Sigma_{u_k y_{k|k-1}}\Sigma_{y_{k|k-1}}^{-1}\Sigma_{u_k y_{k|k-1}}^{T} = \Sigma_{u_{k|k-1}} - L_{u_k}\left(\Sigma_{u_{k|k-1}}D^T + \Sigma_{u_k x_{k|k-1}}C^T\right)^T \tag{23}$$

$$\Sigma_{x_k u_{k|k}} = \Sigma_{x_k u_{k|k-1}} - \Sigma_{x_k y_{k|k-1}}\Sigma_{y_{k|k-1}}^{-1}\Sigma_{u_k y_{k|k-1}}^{T} = \Sigma_{x_k u_{k|k-1}} - \left(\Sigma_{x_{k|k-1}}C^T + \Sigma_{x_k u_{k|k-1}}D^T\right)L_{u_k}^T \tag{24}$$

3.2. Time update of state and input

Time update of state is straightforward using linear transformation. Based on Eq. (1), the state at time step k can be re-written in the following form

$$x_{k+1} = [A \quad B \quad I]\begin{Bmatrix}x_k\\u_k\\w_k\end{Bmatrix} \tag{25}$$

Because the linear transformation in Eq. (25) has full row-rank, the estimate of x_{k+1} given y_k^{seq} can thus be written as

$$\hat{x}_{k+1|k} = \mathbb{E}\left(x_{k+1}\middle|y_k^{\text{seq}}\right) = [A \quad B \quad I]\mathbb{E}\left(\begin{Bmatrix}x_k\\u_k\\w_k\end{Bmatrix}\middle|y_k^{\text{seq}}\right) = A\hat{x}_{k|k} + B\hat{u}_{k|k} \tag{26}$$

Here $\mathbb{E}\left(w_k\middle|y_k^{\text{seq}}\right) = 0$ because process noise w_k is independent from y_k^{seq} (Eq. (8)). The conditional covariance is given by

$$\Sigma_{x_{k+1|k}} \triangleq \mathrm{cov}\left(x_{k+1}\middle|y_k^{\mathrm{seq}}\right) = \begin{bmatrix} A & B & I \end{bmatrix} \begin{bmatrix} \Sigma_{x_{k|k}} & \Sigma_{x_k u_{k|k}} & 0 \\ \Sigma_{u_k x_{k|k}} & \Sigma_{u_{k|k}} & 0 \\ 0 & 0 & \Sigma_w \end{bmatrix} \begin{bmatrix} A^T \\ B^T \\ I \end{bmatrix}$$

$$= \begin{bmatrix} A & B \end{bmatrix} \begin{bmatrix} \Sigma_{x_{k|k}} & \Sigma_{x_k u_{k|k}} \\ \Sigma_{u_k x_{k|k}} & \Sigma_{u_{k|k}} \end{bmatrix} \begin{bmatrix} A^T \\ B^T \end{bmatrix} + \Sigma_w \tag{27}$$

Note here because the process noise w_k is independent from x_k, u_k and y_k^{seq}, the cross-covariance of state-noise and input-noise are zero, i.e. $\Sigma_{x_k w_{k|k}} = 0$ and $\Sigma_{u_k w_{k|k}} = 0$. In addition, $\mathrm{cov}\left(w_k\middle|y_k^{\mathrm{seq}}\right) = \mathrm{cov}(w_k) = \Sigma_w$.

In terms of time update of input, a state space model of the input can be used to propagate the input over time. When a Gaussian random walk model is assumed as $u_{k+1} = u_k + \xi_k$ with $\xi_k \sim \mathcal{N}(0, \Sigma_\xi)$, the conditional expectation and covariance are

$$\hat{u}_{k+1|k} \triangleq \mathbb{E}\left(u_{k+1}\middle|y_k^{\mathrm{seq}}\right) = \mathbb{E}\left(u_k + \xi_k\middle|y_k^{\mathrm{seq}}\right) = \hat{u}_{k|k} \tag{28}$$

$$\Sigma_{u_{k+1|k}} \triangleq \mathrm{cov}\left(u_{k+1}\middle|y_k^{\mathrm{seq}}\right) = \mathrm{cov}\left(u_k + \xi_k\middle|y_k^{\mathrm{seq}}\right) = \Sigma_{u_{k|k}} + \Sigma_\xi \tag{29}$$

$$\Sigma_{x_{k+1}u_{k+1|k}} \triangleq \mathrm{cov}\left(x_{k+1}, u_{k+1}\middle|y_k^{\mathrm{seq}}\right) = \mathrm{cov}\left(Ax_k + Bu_k + w_k, u_k + \xi_k\middle|y_k^{\mathrm{seq}}\right) = A\Sigma_{x_k u_{k|k}} + B\Sigma_{u_{k|k}} \tag{30}$$

This approach is the same as augmenting the state vector with the unknown input; the resulting augmented state can then be estimated using a regular Kalman filter [10]. Hereinafter, this estimator with a Gaussian random walk input model is referred to as the augmented Kalman filter (AKF). The resulting augmented system is found to suffer from un-observability issue when only acceleration measurements are available [10]. To resolve the issue, u_k can be assumed to be zero-mean white Gaussian with $u_k \sim \mathcal{N}(0, \Sigma_u)$. With this assumption, u_k is independent from x_0, u_{k-1}^{seq}, w_{k-1}^{seq} and v_{k-1}^{seq}. Therefore, based on Eq. (7) and Eq. (8), u_{k+1} is independent from x_{k+1} and y_k^{seq}. As a result,

$$\hat{u}_{k+1|k} \triangleq \mathbb{E}\left(u_{k+1}\middle|y_k^{\mathrm{seq}}\right) = \mathbb{E}(u_{k+1}) = 0 \tag{31}$$

$$\Sigma_{u_{k+1|k}} \triangleq \mathrm{cov}\left(u_{k+1}\middle|y_k^{\mathrm{seq}}\right) = \Sigma_u \tag{32}$$

$$\Sigma_{x_{k+1}u_{k+1|k}} \triangleq \mathrm{cov}\left(x_{k+1}, u_{k+1}\middle|y_k^{\mathrm{seq}}\right) = \Sigma_{u_{k+1}x_{k+1|k}}^T = 0 \tag{33}$$

Hereinafter, this estimator with a finite input covariance Σ_u is referred to as the finite input covariance (FIC) estimator. Up to here, simultaneous estimation of the state and input given y_k^{seq} have been derived based on the

unifying MMSE framework, and the difference between AKF and FIC is shown to be in the time update stage. Table 1 summarizes the AKF and the proposed FIC using the time updated priors given by Eq. (31) ~ (33).

Table 1 Input-state estimation using the augmented Kalman filter and finite input covariance estimator

Augmented Kalman filter (AKF)		Finite input covariance (FIC) estimator	
Initialization:			
$\hat{x}_{0\|-1} = \mu_{x_0}, \Sigma_{x_{0\|-1}} = \Sigma_{x_0}, \hat{u}_{0\|-1} = \hat{u}_0, \Sigma_{u_{0\|-1}} = \Sigma_{u_0}, \Sigma_{x_0 u_{0\|-1}} = \Sigma_{x_0 u_0}$		$\hat{x}_{0\|-1} = \mu_{x_0}, \ \Sigma_{x_{0\|-1}} = \Sigma_{x_0}$	
`for` $k = 0, 1, \ldots, n$			
Measurement update of input:			
$\Sigma_{y_{k\|k-1}} = C\Sigma_{x_{k\|k-1}}C^T + D\Sigma_{u_{k\|k-1}}D^T + \Sigma_v + D\Sigma_{u_k x_{k\|k-1}}C^T + C\Sigma_{x_k u_{k\|k-1}}D^T$	Rept. (16)	$\Sigma_{y_{k\|k-1}} = C\Sigma_{x_{k\|k-1}}C^T + D\Sigma_u D^T + \Sigma_v$	(34)
$L_{u_k} = \left(\Sigma_{u_{k\|k-1}}D^T + \Sigma_{u_k x_{k\|k-1}}C^T\right)\Sigma_{y_{k\|k-1}}^{-1}$	Rept. (20)	$L_{u_k} = \Sigma_u D^T \Sigma_{y_{k\|k-1}}^{-1}$	(35)
$\hat{u}_{k\|k} = \hat{u}_{k\|k-1} + L_{u_k}\left(y_k - C\hat{x}_{k\|k-1} - D\hat{u}_{k\|k-1}\right)$	Rept. (18)	$\hat{u}_{k\|k} = L_{u_k}\left(y_k - C\hat{x}_{k\|k-1}\right)$	(36)
$\Sigma_{u_{k\|k}} = \Sigma_{u_{k\|k-1}} - L_{u_k}\left(\Sigma_{u_{k\|k-1}}D^T + \Sigma_{u_k x_{k\|k-1}}C^T\right)^T$	Rept. (23)	$\Sigma_{u_{k\|k}} = \Sigma_u - L_{u_k}D\Sigma_u$	(37)
$\Sigma_{x_k u_{k\|k}} = \Sigma_{x_k u_{k\|k-1}} - \left(\Sigma_{x_{k\|k-1}}C^T + \Sigma_{x_k u_{k\|k-1}}D^T\right)L_{u_k}^T$	Rept. (24)	$\Sigma_{x_k u_{k\|k}} = -\Sigma_{x_{k\|k-1}}C^T L_{u_k}^T$	(38)
Measurement update of state:			
$L_{x_k} = \left(\Sigma_{x_{k\|k-1}}C^T + \Sigma_{x_k u_{k\|k-1}}D^T\right)\Sigma_{y_{k\|k-1}}^{-1}$	Rept. (19)	$L_{x_k} = \Sigma_{x_{k\|k-1}}C^T\Sigma_{y_{k\|k-1}}^{-1}$	(39)
$\hat{x}_{k\|k} = \hat{x}_{k\|k-1} + L_{x_k}\left(y_k - C\hat{x}_{k\|k-1} - D\hat{u}_{k\|k-1}\right)$	Rept. (18)	$\hat{x}_{k\|k} = \hat{x}_{k\|k-1} + L_{x_k}\left(y_k - C\hat{x}_{k\|k-1}\right)$	(40)
$\Sigma_{x_{k\|k}} = \Sigma_{x_{k\|k-1}} - L_{x_k}\left(\Sigma_{x_{k\|k-1}}C^T + \Sigma_{x_k u_{k\|k-1}}D^T\right)^T$	Rept. (22)	$\Sigma_{x_{k\|k}} = \Sigma_{x_{k\|k-1}} - L_{x_k}C\Sigma_{x_{k\|k-1}}$	(41)
Time update of state:			
$\hat{x}_{k+1\|k} = A\hat{x}_{k\|k} + B\hat{u}_{k\|k}$			Rept. (26)
$\Sigma_{x_{k+1\|k}} = [A \quad B]\begin{bmatrix}\Sigma_{x_{k\|k}} & \Sigma_{x_k u_{k\|k}} \\ \Sigma_{u_k x_{k\|k}} & \Sigma_{u_{k\|k}}\end{bmatrix}\begin{bmatrix}A^T \\ B^T\end{bmatrix} + \Sigma_w$			Rept. (27)
Time update of input:			
$\hat{u}_{k+1\|k} = \hat{u}_{k\|k}$	Rept. (28)	$\hat{u}_{k+1\|k} = 0$	Rept. (31)
$\Sigma_{u_{k+1\|k}} = \Sigma_{u_{k\|k}} + \Sigma_\xi$	Rept. (29)	$\Sigma_{u_{k+1\|k}} = \Sigma_u$	Rept. (32)
$\Sigma_{x_{k+1}u_{k+1\|k}} = A\Sigma_{x_k u_{k\|k}} + B\Sigma_{u_{k\|k}}$	Rept. (30)	$\Sigma_{x_{k+1}u_{k+1\|k}} = 0$	Rept. (33)
`end`			

3.3. Measurement update with large and infinite input covariance

Equation (34) may be ill-conditioned when the input covariance Σ_u is much larger than the state estimation covariance and $D\Sigma_u D^T$ does not have full rank. To improve the conditioning of Eq. (34), define a symmetric positive definite matrix as:

$$\Sigma_{\tilde{y}_{k|k-1}} \triangleq C\Sigma_{x_{k|k-1}}C^T + \Sigma_v \tag{42}$$

Based on the matrix push through identity in Lemma 1, input estimation gain L_{u_k} from Eq. (35) can be modified as

$$L_{u_k} = \Sigma_u D^T \left(\Sigma_{\tilde{y}_{k|k-1}} + D\Sigma_u D^T\right)^{-1} = \Sigma_u D^T \left(I + \Sigma_{\tilde{y}_{k|k-1}}^{-1} D\Sigma_u D^T\right)^{-1} \Sigma_{\tilde{y}_{k|k-1}}^{-1}$$

$$= \left(\Sigma_u^{-1} + D^T \Sigma_{\tilde{y}_{k|k-1}}^{-1} D\right)^{-1} D^T \Sigma_{\tilde{y}_{k|k-1}}^{-1} \tag{43}$$

The corresponding input estimation error covariance in Eq. (37) can be modified using Eq. (4a) in Lemma 2 as

$$\Sigma_{u_{k|k}} = \Sigma_u - \Sigma_u D^T \Sigma_{y_{k|k-1}}^{-1} D\Sigma_u = \left(\Sigma_u^{-1} + D^T \Sigma_{\tilde{y}_{k|k-1}}^{-1} D\right)^{-1} \tag{44}$$

To improve the ill-conditioning of $\Sigma_{y_{k|k-1}}$ caused by the term $D\Sigma_u D^T$, the matrix inversion $\Sigma_{y_{k|k-1}}^{-1}$ in Eq. (39) can be rewritten as

$$\Sigma_{y_{k|k-1}}^{-1} = \left(\Sigma_{\tilde{y}_{k|k-1}} + D\Sigma_u D^T\right)^{-1} = \Sigma_{\tilde{y}_{k|k-1}}^{-1} \left(I - D\left(\Sigma_u^{-1} + D^T \Sigma_{\tilde{y}_{k|k-1}}^{-1} D\right)^{-1} D^T \Sigma_{\tilde{y}_{k|k-1}}^{-1}\right) \tag{45}$$

Therefore, an equivalent set of equations given by Eq. (43), (44) and (45) can be used to modify Eq. (35), (37) and (39) to improve the condition of Eq. (34) in the FIC estimator.

Furthermore, if the unknown input is highly uncertain such that no prior knowledge can be used to estimate u_k, $\Sigma_{u_{k|k-1}} = \Sigma_u$ can be replaced with Σ_∞, which denotes a diagonal matrix with diagonal entries being infinity. When the number of unknown inputs is smaller than the number of measurements, i.e. D has full column rank ($n_u \leq m$ and $\text{rank}(D) = n_u$), $\Sigma_u^{-1} = \Sigma_\infty^{-1} = 0$ in Eq. (43) ~ (45) can be eliminated, resulting in Eq. (46) ~ (48) as follows.

$$L_{u_k} = \left(D^T \Sigma_{\tilde{y}_{k|k-1}}^{-1} D\right)^{-1} D^T \Sigma_{\tilde{y}_{k|k-1}}^{-1} = \Sigma_{u_{k|k}} D^T \Sigma_{\tilde{y}_{k|k-1}}^{-1} \tag{46}$$

$$\Sigma_{u_{k|k}} = \left(D^T \Sigma_{\tilde{y}_{k|k-1}}^{-1} D\right)^{-1} \tag{47}$$

$$\Sigma_{y_{k|k-1}}^{-1} = \Sigma_{\tilde{y}_{k|k-1}}^{-1} \left(I - D\left(D^T \Sigma_{\tilde{y}_{k|k-1}}^{-1} D\right)^{-1} D^T \Sigma_{\tilde{y}_{k|k-1}}^{-1}\right) = \Sigma_{\tilde{y}_{k|k-1}}^{-1} \left(I - DL_{u_k}\right) \tag{48}$$

As a result of (48), the state estimation gain in (39) can be rewritten as

$$L_{x_k} = \Sigma_{x_{k|k-1}} C^T \Sigma_{y_{k|k-1}}^{-1} = \Sigma_{x_{k|k-1}} C^T \Sigma_{\tilde{y}_{k|k-1}}^{-1} \left(I - DL_{u_k}\right) \tag{49}$$

To summarize, when assuming $\Sigma_u = \Sigma_\infty$ and D has full column rank, Eq. (34), (35), (37) and (39) in Table 1 can be replaced by Eq. (42), (46), (47) and (49). Time update of the state is the same as Eq. (26) and (27), and time update of input remains the same as in Eq. (32) and (33) for the FIC estimator .

Theorem When the input covariance Σ_u of the FIC estimator approaches infinity (Σ_∞) and the feedthrough matrix D has full column rank, the FIC estimator with L_{u_k}, $\Sigma_{u_{k|k}}$ and L_{x_k} given by Eq. (46), (47) and (49) is equivalent to the WLS estimator proposed by Gillijns and De Moor in [6].

Proof. In comparison to the notations in [6], the symmetric positive definite matrix $\Sigma_{\tilde{y}_{k|k-1}}$ defined here is denoted as $\tilde{R}_k$ in [6]; the input estimation gain L_{u_k} is denoted as M_k; the state estimation gain L_{x_k} is denoted as L_k; and $\Sigma_{x_{k|k-1}} C^T \Sigma^{-1}_{\tilde{y}_{k|k-1}}$ is denoted as K_k. Therefore, Eq. (42), (46), (36) and (47) here are equivalent to the unknown input estimation step in [6]. Substituting L_{x_k} from Eq. (49) into Eq. (40) and (41), the state measurement update step in [6] can be obtained. Finally, Eq. (26) and (27) are equivalent to the time update step in [6]. ■

Hereinafter, the FIC estimator with $\Sigma_u = \Sigma_\infty$ is referred to as the weighted least squares (WLS) estimator. Thus far, the relationship among all three estimators, i.e. AKF, FIC and WLS, has been demonstrated based on the unifying MMSE framework. In theory, neither the FIC nor the AKF assumes the feedthrough matrix D has full column rank. However, to estimate all the unknown inputs accurately, in practice full-column rank of D is needed and the magnitude of Du_k should be relatively large compared to the measurement noise v_k.

4. Numerical example

To compare the performance of the estimators, a state space dynamical model is formulated based on the following equations of motion with n_{DOF} degrees-of-freedom (DOFs):

$$M\ddot{q}(t) + C_{\mathrm{damp}}\dot{q}(t) + Kq(t) = \Gamma_u u(t) \tag{50}$$

where M, K, $C_{\mathrm{damp}} \in \mathbb{R}^{n_{\mathrm{DOF}} \times n_{\mathrm{DOF}}}$ are the mass, stiffness and damping matrices; $q(t)$, $\dot{q}(t)$ and $\ddot{q}(t) \in \mathbb{R}^{n_{\mathrm{DOF}}}$ are displacement, velocity and acceleration vectors at time t; $\Gamma_u \in \mathbb{R}^{n_{\mathrm{DOF}} \times n_u}$ is the input location matrix, with ones at the input DOFs and zeros elsewhere; and $u(t) \in \mathbb{R}^{n_u}$ is the force input. To reformulate Eq. (50) in state space form, define the state vector as $x \triangleq \begin{Bmatrix} q \\ \dot{q} \end{Bmatrix}$ with a length of $n = 2n_{\mathrm{DOF}}$. As a result, the equations of motion can be reformulated in state space as follows, together with corresponding measurement equation for m number of acceleration measurements.

$$\dot{x} = \begin{bmatrix} 0 & I \\ -M^{-1}K & -M^{-1}C_{\text{damp}} \end{bmatrix} x + \begin{bmatrix} 0 \\ M^{-1}\Gamma_u \end{bmatrix} u \triangleq A_c x + B_c u \tag{51}$$

$$y = \Gamma_y \begin{bmatrix} -M^{-1}K & -M^{-1}C_{\text{damp}} \end{bmatrix} x + \Gamma_y M^{-1}\Gamma_u u + v \triangleq C_c x + D_c u + v \tag{52}$$

Here $y \in \mathbb{R}^m$ represents the acceleration measurement; $\Gamma_y \in \mathbb{R}^{m \times n_{\text{DOF}}}$ is the output location matrix; $v \in \mathbb{R}^m$ is the measurement noise; A_c, B_c, C_c and D_c represent the system matrix, input matrix, output matrix and feedthrough matrix of the continuous state space model. In this numerical example, the three estimators shown in Section 3 are validated using a two-story shear structure, i.e. $n_{\text{DOF}} = 2$. The mass and stiffness values are provided in Figure 1 and the resonance frequencies of the structure are 1.67 Hz and 4.5 Hz. A modal damping ratio of 2% is assumed for both modes. The excitation $u(t)$ is applied at the 1st DOF, i.e. at mass m_1.

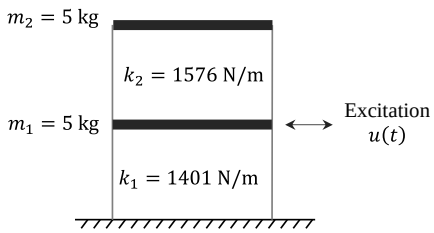

Figure 1 Two-story structural example

The measurement y contains the simulated acceleration response of both DOFs. As a result, the mass, stiffness, damping, input location and output location matrices of this example are

$$M = \begin{bmatrix} 5 & 0 \\ 0 & 5 \end{bmatrix}, \quad K = \begin{bmatrix} 2977 & -1576 \\ -1576 & 1576 \end{bmatrix}, \quad C_{\text{damp}} = \begin{bmatrix} 4.6017 & -1.625 \\ -1.625 & 3.1571 \end{bmatrix}, \quad \Gamma_u = \begin{bmatrix} 1 \\ 0 \end{bmatrix}, \quad \Gamma_y = \begin{bmatrix} 1 & 0 \\ 0 & 1 \end{bmatrix}.$$

Note that in this structural example, the continuous feedthrough matrix $D_c = \Gamma_y M^{-1}\Gamma_u$ has full column rank because the measured DOFs contain the input DOF. In addition, although the input excitation in this example is only applied at the 1st DOF, the estimators can simultaneously estimate inputs at multiple locations if D_c has full column rank. To implement the estimators in discrete time, the continuous-time system given by Eq. (51) and (52) is discretized using zero-order-hold with a time step of 0.005s. The resulting discrete state space matrices A, B, C and D are given as follows

$$A = \begin{bmatrix} 0.993 & 0.004 & 0.005 & 10^{-5} \\ 0.004 & 0.996 & 10^{-5} & 0.005 \\ -2.96 & 1.565 & 0.988 & 0.006 \\ 1.565 & -1.568 & 0.006 & 0.993 \end{bmatrix}, B = \begin{bmatrix} 2.49 \\ 0.003 \\ 995.2 \\ 2.12 \end{bmatrix} \times 10^{-6}, C = \begin{bmatrix} -595.4 & 315.2 & -0.92 & 0.325 \\ 315.2 & -315.2 & 0.325 & -0.631 \end{bmatrix}, \; D = \begin{bmatrix} 0.2 \\ 0 \end{bmatrix}.$$

To compare the estimator performance, two types of input excitations are considered here. The first type is a white Gaussian input excitation with a standard deviation of 10 N, i.e. $u_k \sim \mathcal{N}(0, 10^2)$. The second type is a 3 Hz periodic sinusoidal input with a magnitude of 10 N. Note that the sinusoidal input is chosen on purpose such that the white Gaussian noise assumption of the unknown input is violated. The simulated measurements are contaminated by measurement noise with a standard deviation of $\sigma_v = 10^{-3}$ m/s^2 and sampled at 200 Hz. For easier comparison of the input estimators, σ_v values available to the estimators are assumed to be the same as the one used in the simulated measurements. The initial value μ_{x_0} and the diagonal entries of Σ_{x_0} are set as zero for all estimators, assuming the initial condition of the structure is known. Moreover, for the AKF, $\hat{u}_0$, Σ_{u_0} and $\Sigma_{x_0 u_0}$ are set as zero.

4.1. Effect of covariance knowledge on input estimation

In practice, the actual input covariance Σ_u and process noise covariance Σ_w are often unknown, while the measurement noise covariance Σ_v can be approximated based on sensor noise level, as well as any uncertainty present in the measurement equation. Knowledge of the covariances Σ_u and Σ_w by an estimator can have significant effect on the estimation performance. To study such effects, numerical simulations are performed first, where the actual/true values of these covariances are known. When generating time history data, the true input covariance and process noise covariance used in the dynamics simulation are denoted $\Sigma_{u,sim}$ and $\Sigma_{w,sim}$, respectively. During estimation, all three estimators (FIC, AKF and WLS) require a value of process noise covariance Σ_w; the value available to the estimator is thus denoted $\Sigma_{w,est}$. The FIC estimator requires a value of the input covariance (see Table 1); the value available to the estimator is denoted $\Sigma_{u,est}$. Similarly, operation of the AKF estimator requires the random walk covariance Σ_ξ (also see Table 1); accordingly, the value is denoted $\Sigma_{\xi,est}$. On the other hand, operation of the WLS estimation does not require any input covariance Σ_u, as shown in Eq. (46) ~ (48). In summary, the covariances for the estimator operation include $\Sigma_{u,est}$ of the FIC estimator, $\Sigma_{\xi,est}$ of the AKF, and $\Sigma_{w,est}$ and $\Sigma_{v,est}$ for all three estimators. Table 2 summarizes the data generation process and the estimator covariances during each trial run.

Table 2 Summary of data generation and estimator covariances

Covariances	Time history generation	Estimation		
		FIC	AKF	WLS
Input	(1) White noise $\Sigma_{u,\,sim} = 100\ \mathrm{N}^2$ (2) Sinusoidal input	$\Sigma_{u,\,est}$ (1 to $10^7\ \mathrm{N}^2$)	$\Sigma_{\xi,est}$ (1 to $10^7\ \mathrm{N}^2$)	-
Initial state	Static	$\mu_{x_0} = 0,\ \Sigma_{x_0} = 0$		
Process noise	$\Sigma_{w,\,sim} = 0$ or $10^{-10}I$	$\Sigma_{w,\,est} = 0$		
Measurement noise	$\Sigma_{v,\,sim} = 10^{-6}\ (\mathrm{m/s^2})^2$	$\Sigma_{v,\,est} = 10^{-6}\ (\mathrm{m/s^2})^2$		

To study estimator covariance effects under white Gaussian excitation, 50 independent runs of dynamics simulation are performed using randomly generated 30 seconds of input u_k (with $\Sigma_{u,sim} = 100\mathrm{N}^2$) and measurement noise v_k. Using data from each trial run, the root mean square (RMS) error e_u can be calculated based on the estimated input $\hat{u}_k$ and the actual input u_k, defined as $e_u \triangleq \sqrt{\frac{1}{\mathbb{K}}\sum_{k=1}^{\mathbb{K}}|u_k - \hat{u}_k|^2}$, where $\mathbb{K}$ is the total number of data points. Because all three estimators require process noise covariance $\Sigma_{w,est}$, the same value is used when performing estimation by all estimators and for 50 trials. When performing estimation for each trial run, the WLS estimator is operated only once, because the estimator does not require knowledge of input covariance $\Sigma_{u,est}$ or $\Sigma_{\xi,est}$; the averaged RMS error among 50 trials is then obtained as $\bar{e}_u = \frac{1}{n_{trial}}\sum_{i=1}^{n_{trial}} e_u^{(i)}$. On the other hand, the FIC estimator is performed for different values of $\Sigma_{u,est}$ ranging from 1 to $10^7\ \mathrm{N}^2$. At each value of $\Sigma_{u,est}$, one estimation time history $\hat{u}_k$ is generated and e_u is calculated accordingly for one trial; among 50 trials the averaged RMS $\bar{e}_u$ is obtained. Thus, the results provide the relationship between $\bar{e}_u$ and $\Sigma_{u,est}$. Likewise, the AKF estimator is performed for different values of $\Sigma_{\xi,est}$ in the same range of 1 to $10^7\ \mathrm{N}^2$. After averaging among 50 trials, the relationship between $\bar{e}_u$ and $\Sigma_{\xi,est}$ can be obtained. When no process noise is added to the system in all 50 trials, i.e. $\Sigma_{w,sim} = 0$, Figure 2(a) shows the change in $\bar{e}_u$ as $\Sigma_{u,est}$ of FIC and $\Sigma_{\xi,est}$ of AKF vary with $\Sigma_{w,est} = 0$. The smallest RMS error is achieved by the FIC estimator when $\Sigma_{u,est}$ is very close to the actual input covariance $\Sigma_{u,sim} = 100\ \mathrm{N}^2$. It is also observed that AKF is not sensitive to the change of $\Sigma_{\xi,est}$ and has a similar averaged RMS error as the WLS estimator, resulting in the coinciding curves in Figure 2(a). Specifically, the averaged RMS from both AKF and WLS estimator is around 0.42 N, and the smallest averaged RMS achieved by FIC is around 0.25 N. In addition, the RMS error of the FIC estimator is smaller than both the AKF and WLS when $\Sigma_{u,est}$ is in the range from 5 to $10^5\ \mathrm{N}^2$. As $\Sigma_{u,est}$

becomes larger than 10^6 N^2, the FIC estimator converges to the WLS estimator, which is consistent with the theorem in Section 3.

To investigate the situation when process noise covariance is not exactly known, a small amount of process noise is randomly generated in each of the 50 trial runs, while the estimators assume no process noise is present and the system model is accurate. Figure 2(b) illustrates the averaged RMS errors of estimated input given each $\Sigma_{u,est}$ and $\Sigma_{\xi,est}$ when $\Sigma_{w,sim} = 10^{-10}I$ and $\Sigma_{w,est} = 0$. For the AKF and WLS estimator, the averaged input RMS error increase significantly to around 1.90 N, while the FIC estimator is able to achieve a much smaller RMS error of 0.5 N when $\Sigma_{u,est}$ is chosen around 5 N^2. The best choice of $\Sigma_{u,est}$ here is smaller than $\Sigma_{u,sim} = 100$ N^2, when the $\Sigma_{w,est}$ used by the FIC estimator is smaller than the actual $\Sigma_{w,sim}$ used for simulation. In addition, the RMS error from FIC estimator is always smaller than AKF and WLS estimator when $\Sigma_{u,est}$ ranges from 1 to 10^5 N^2.

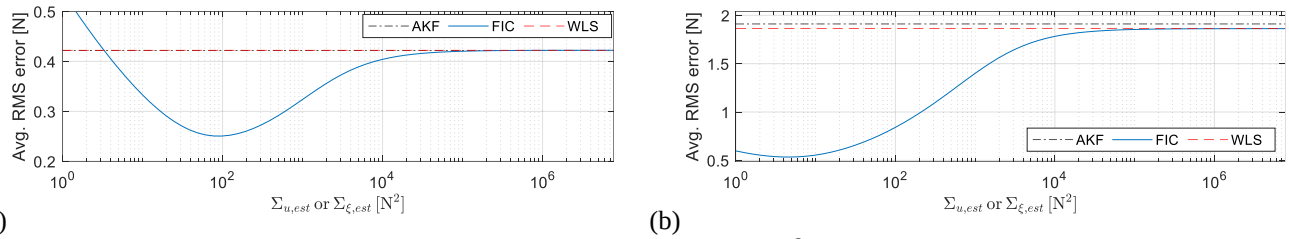

(a) (b)

Figure 2 Averaged RMS error $\bar{e}_u$ of white input estimation ($\Sigma_{u,sim} = 100\mathrm{N}^2$): (a) $\Sigma_{w,sim} = \Sigma_{w,est} = 0$ (results from AKF and WLS estimator coincide); (b) $\Sigma_{w,sim} = 10^{-10}I, \Sigma_{w,est} = 0$

Next, a sinusoidal input excitation is adopted here on purpose to violate the white Gaussian assumption of the unknown input. Using the 3 Hz periodic sinusoidal input excitation with a magnitude of 10 N, 50 independent runs of 15 seconds dynamics simulation with randomly generated white Gaussian process noise and measurement noise are performed. Same as in the white Gaussian input simulation, the input RMS error e_u is calculated in each trial run for different values of $\Sigma_{u,est}$ and $\Sigma_{\xi,est}$ ranging from 1 to 10^7 N^2. After averaging among 50 trials, the relationship between $\bar{e}_u$ and $\Sigma_{u,est}$ of the FIC estimator can be obtained. Likewise, the relationship between $\bar{e}_u$ and $\Sigma_{\xi,est}$ of the AKF is obtained in the same manner. Figure 3(a) shows the change in $\bar{e}_u$ as $\Sigma_{u,est}$ and $\Sigma_{\xi,est}$ vary, when there is no process noise added to the system in all 50 trials, i.e. $\Sigma_{w,sim} = 0$. Accordingly, all estimators use $\Sigma_{w,est} = 0$. The smallest RMS error $\bar{e}_u$ is achieved by the FIC estimator when $\Sigma_{u,est}$ is around 25 N^2, when the actual calculated input covariance $\Sigma_{u,sim}$ is 50 N^2. The best $\Sigma_{u,est}$ of FIC does not equal to the actual $\Sigma_{u,sim}$, which is as expected

because the input signal is not white noise as assumed. However, compared to the AKF and WLS estimator, smaller RMS error can still be achieved by the FIC estimator when $\Sigma_{u,est}$ is within a large range around the actual $\Sigma_{u,sim}$. In addition, AKF is not sensitive to the changes of $\Sigma_{\xi,est}$ and has an averaged RMS error around 0.45 N, leading to the results coinciding with the WLS estimator in Figure 3(a). To investigate the situation when process noise covariance is not exactly known under sinusoidal excitation, a small amount of process noise with covariance $\Sigma_{w,sim} = 10^{-10}I$ is added to the system while the estimators assume $\Sigma_{w,est} = 0$. For the AKF and WLS estimator, $\bar{e}_u$ increases significantly to 1.94 N, while the FIC estimator is again able to achieve a much smaller error of 0.4 N when $\Sigma_{u,est}$ is around 3 N^2. In addition, the error $\bar{e}_u$ from the FIC estimator is always smaller than the AKF and WLS estimator when $\Sigma_{u,est}$ ranges from 1 to 10^5 N^2.

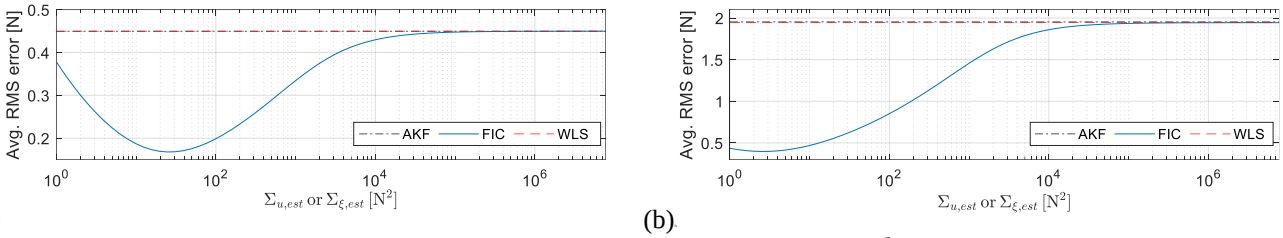

Figure 3 Averaged input RMS error $\bar{e}_u$ of sinusoidal input estimation ($\Sigma_{u,sim} = 50\mathrm{N}^2$): (a) $\Sigma_{w,sim} = \Sigma_{w,est} = 0$ (AKF and WLS coincide); (b) $\Sigma_{w,sim} = 10^{-10}I, \Sigma_{w,est} = 0$ (AKF and WLS coincide)

To summarize, the best choice of $\Sigma_{u,est}$ for the FIC estimator is found to be directly related to the prior statistical property for the type of input expected in certain application. It is also worth noting that for all cases presented thus far, the FIC estimator converges to the WLS estimator when $\Sigma_{u,est}$ is large, regardless of input types or covariances available to the estimator. In addition, if $\Sigma_{w,est}$ is smaller than the actual $\Sigma_{w,sim}$, the best choice of $\Sigma_{u,est}$ of the FIC estimator will be slightly smaller than $\Sigma_{u,sim}$, and vice versa. The difference in RMS error between AKF and WLS is relatively small compared to FIC estimation. This is partially due to the drift error when only acceleration measurements are available, which will be shown in the following subsection. Furthermore, by varying $\Sigma_{\xi,est}$ of the AKF, the performance could not be improved as much as the FIC estimator.

4.2. Simultaneous input-state estimation

This subsection first compares the time history of the estimated inputs for a single run of white Gaussian excitation for 60 seconds. Recall that the input has a standard deviation of 10 N, i.e. the input covariance $\Sigma_{u,sim} = 100$ N^2. The

simulated process noise is set as 0, i.e. $\Sigma_{w,sim} = 0$. Based on the discussion on white noise excitation in Section 4.1, $\Sigma_{\xi,est}$ of AKF and $\Sigma_{u,est}$ of FIC are set as 100 N^2. The process noise covariance $\Sigma_{w,est}$ for all estimators is set as 0, same as $\Sigma_{w,sim}$. The simulated acceleration response is contaminated with measurement noise of $\sigma_{v,sim} = 10^{-2}\ \mathrm{m/s^2}$, which corresponds to 0.4% of the acceleration response intensity at the 1st DOF and 0.7% of the acceleration response intensity at the 2nd DOF. Accordingly, measurement noise covariance is set as $\Sigma_{v,est} = \Sigma_{v,sim} = 10^{-4} I\ (\mathrm{m/s^2})^2$. The same initialization of state and the corresponding state estimation covariance is used, which assumes the initial condition is static and known. It is observed that all estimators perform almost equally well during the initial time period but the AKF and WLS start to drift slightly over time. Figure 4(a) ~ (c) show the close-up plots of AKF, WLS and FIC estimation results during the final 0.5s, respectively. The confidence interval of three times square root of input estimation error covariance, $\pm 3\sigma_{u_{k|k}}$, is included in the close-up plots for the estimated input $\hat{u}_{k|k}$ obtained from each estimator. It can be seen that the FIC estimator performs consistently well over time with a tight confidence interval (Figure 4(c)), while both the AKF and WLS estimators cannot provide a good estimate of the input as time increases (Figure 4(a) and (b)). In addition, Figure 4(d) shows the time history of input estimation error covariance $\Sigma_{u_{k|k}}$ of FIC and WLS estimation in logarithmic scale. AKF has almost identical result as the WLS estimator and thus is not included in the plots. The input estimation error covariance of the WLS estimator is not able to converge to steady state, while the error covariance of the FIC estimator converges to steady state after 10s. Similar phenomenon can be observed in state estimation. Figure 4(e) shows the state estimation covariance $\Sigma_{x_{k|k}}$ of x_1 and x_2 in logarithmic scale, and Figure 4(f) shows $\Sigma_{x_{k|k}}$ of x_3 and x_4. For the WLS estimator, the error covariance of x_1 and x_2 cannot converge to steady state, while the error covariance of x_3 and x_4 are able to converge after around 9s. For the FIC estimator, the error covariance of all four states can converge to steady state within 10s.

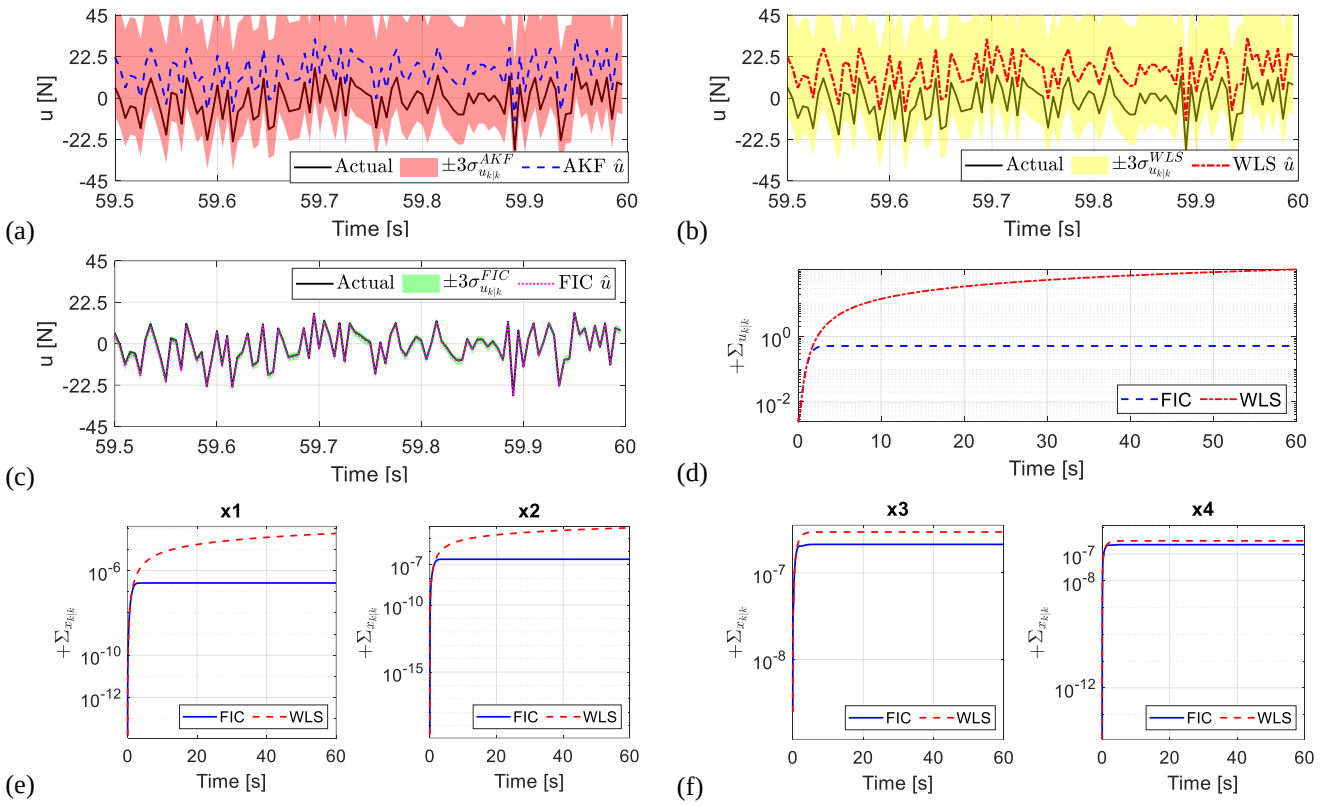

Figure 4 Estimation of white Gaussian input: (a) 59.5~60s of AKF estimation results; (b) 59.5~60s of WLS estimation results; (c) 59.5~60 of FIC estimation results; (d) input estimation error covariance $\Sigma_{u_{k|k}}$; (e) state estimation error covariance $\Sigma_{x_{k|k}}$ of $\hat{x}_1$ and $\hat{x}_2$; (f) state estimation error covariance $\Sigma_{x_{k|k}}$ of $\hat{x}_3$ and $\hat{x}_4$

Next for a single run of sinusoidal excitation, the same 3 Hz sinusoidal input with an amplitude of 10 N is again applied for 15 seconds. The simulated acceleration response is contaminated with measurement noise of $\sigma_{v,sim} = 10^{-2}\ \mathrm{m/s^2}$, which corresponds to 2.6% of the acceleration response intensity at the 1st DOF and 0.7% of the acceleration response intensity at the 2nd DOF. Because the dynamical state space system is accurate and no modeling error is assumed in this example, process noise covariance $\Sigma_{w,est}$ is set as 0. From the discussion on sinusoidal excitation in Section 4.1 when no process is applied to the system, $\Sigma_{\xi,est}$ of AKF and $\Sigma_{u,est}$ of FIC are set as 25 $\mathrm{N^2}$. Because all estimators perform almost equally well during the initial time period, plots are not included here. Figure 5(a) ~ (c) shows the comparison of estimated sinusoidal input from the AKF, WLS and FIC estimators during the final 0.5s, respectively. The confidence interval of three times square root of input estimation error covariance, $\pm 3\sigma_{u_{k|k}}$, is included in the close-up plots for the estimated input $\hat{u}_{k|k}$ obtained from each estimator.

Similar as in the white noise input estimation, the drift phenomenon of the AKF and WLS estimator still exists under sinusoidal input. On the other hand, Figure 5(c) shows that even though the white Gaussian assumption is violated because of the sinusoidal input, the FIC estimator can still estimate the input consistently well over time. Figure 5(d) plots the input estimation error covariance $\Sigma_{u_{k|k}}$ of the FIC and WLS estimator in logarithmic scale (AKF has almost the same result as WLS and thus is not included here). The input estimation error covariance $\Sigma_{u_{k|k}}$ of the WLS estimator cannot converge to steady state, while $\Sigma_{u_{k|k}}$ of the FIC estimator converges after 2.5s. Indeed, not only the input error covariance $\Sigma_{u_{k|k}}$ but also the state estimation error covariance $\Sigma_{x_{k|k}}$ of x_1 and x_2 from the WLS estimator cannot converge to steady state (Figure 5(e)), although the error covariances of x_3 and x_4 are able to converge. In contrast, the state estimation error covariances of all states from the FIC estimator converge to steady state within 2.5s.

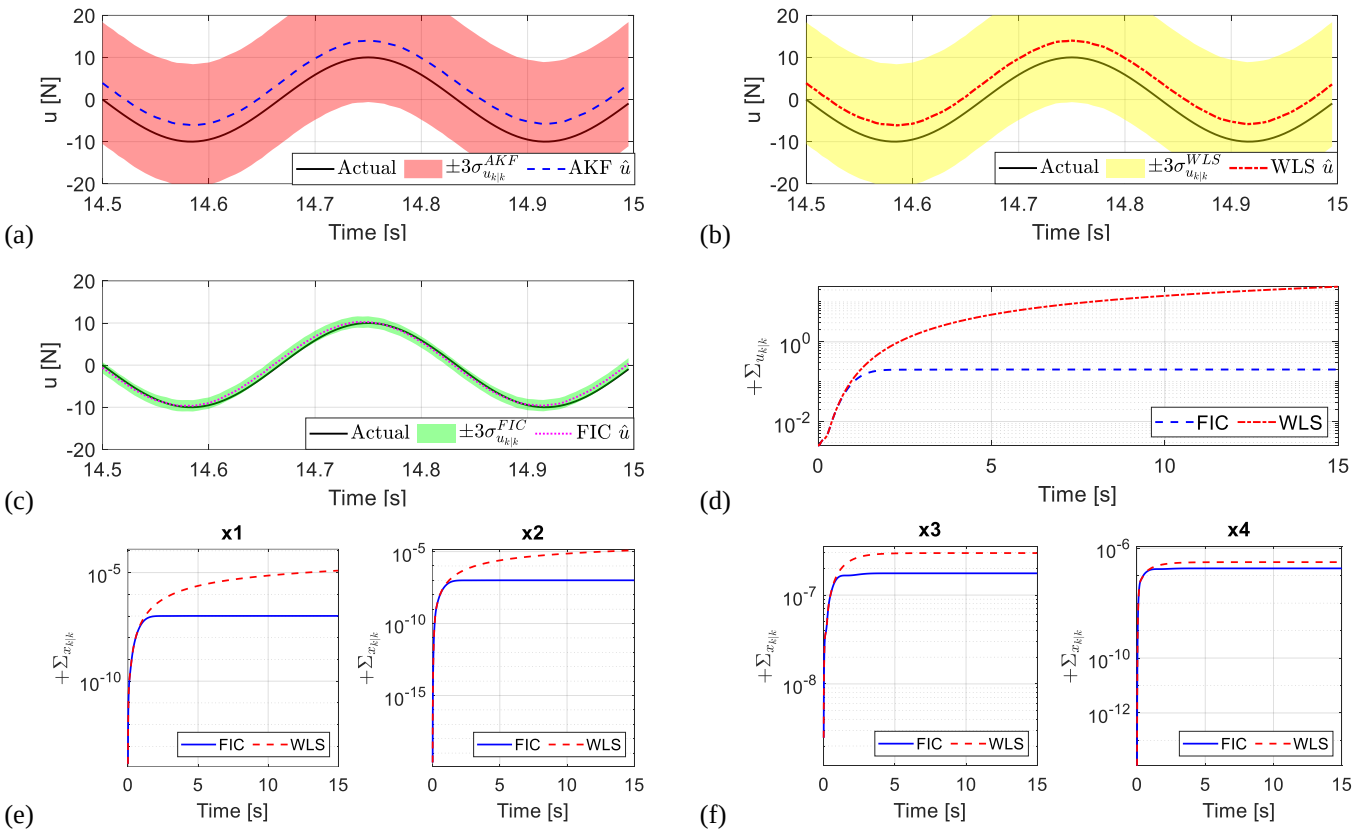

Figure 5 Estimation of sinusoidal input: (a) 14.5~15s of AKF estimation results; (b) 14.5~15s of WLS estimation results; (c) 14.5~15s of FIC estimation results; (d) input estimation error covariance $\Sigma_{u_{k|k}}$; (e) state estimation error covariance $\Sigma_{x_{k|k}}$ of $\hat{x}_1$ and $\hat{x}_2$; (f) state estimation error covariance $\Sigma_{x_{k|k}}$ of $\hat{x}_3$ and $\hat{x}_4$

To quantify the performance of the estimators, the corresponding RMS error of input and displacement estimation from one trial of the white noise input and one trial of the sinusoidal input is summarized in Table 3. For white Gaussian input, the RMS error is calculated for the entire time history, the initial 1s and the final 1s. While all the three estimators achieve similar RMS error during the initial 1s, the FIC estimator performs consistently better in the long run. During the 59~60s, the AKF and WLS estimator have a much larger RMS error in both estimated input and displacement compared to the FIC estimator. For sinusoidal excitation, the RMS error is calculated for the entire time history, the initial 5s and the final 5s. Similar phenomenon can be observed. All three estimators perform equally well during the initial 5s but the errors of AKF and WLS increase as simulation time increases. In all cases, the FIC estimator achieves smallest RMS error (with a small $\Sigma_{u_{k|k}}$) not only in input estimation but also in displacement estimation and eliminates the drift error. Similar results exist in velocity estimation, which is not included here.

Table 3 RMS error comparison among different input estimators

Estimator type		White Gaussian input excitation			Sinusoidal input excitation		
		0~60s	0~1s	59~60s	0~15s	0~5s	10~15s
Input estimation errors (unit: N)	AKF	9.53	0.133	16.35	1.867	0.573	2.410
	WLS	9.52	0.137	16.33	1.871	0.585	2.393
	FIC	0.82	0.120	1.011	0.618	0.477	0.656
Displacement estimation errors (unit: m)	AKF	6.80×10^{-3}	8.81×10^{-5}	1.17×10^{-2}	1.33×10^{-3}	1.03×10^{-3}	1.72×10^{-3}
	WLS	6.79×10^{-3}	9.16×10^{-5}	1.17×10^{-2}	1.33×10^{-3}	1.04×10^{-3}	1.70×10^{-3}
	FIC	5.84×10^{-4}	7.88×10^{-5}	7.14×10^{-4}	4.38×10^{-4}	3.91×10^{-4}	4.67×10^{-4}

The FIC estimator has also been tested with impact load estimation, while the results are omitted due to page limit. Although the FIC estimator is derived based on white Gaussian assumption of the input, the estimator can still provide adequate accuracy for estimating impact load. In particular, better performance can be achieved when the input covariance is chosen such that the corresponding standard deviation is closer to the impact magnitude.

5. Full-scale structural validation

A full-scale structure is used to validate the proposed FIC estimator and compare its performance with the AKF and WLS estimator, when only acceleration measurements are available. Figure 6 shows a set of four identical two-story two-bay concrete frames, which were used to compare different seismic retrofitting approaches. Each frame was constructed with a gap from its neighboring frames, allowing free in-plane longitudinal movement and can thus

be tested independently from the other frames. Experimental data from frame #1 is used in this study. Figure 7 shows the frame consists of two stories with a story height of 3.66 meters (12 ft), and two bays with a column spacing of 5.49 meters (18 ft). The width of the two elevated slabs is 2.74 meters (9 ft). To provide excitation, a hydraulic linear inertia shaker was installed at the middle beam-column joint on the roof, i.e. the second elevated slab (Figure 7). The moving mass on the shaker was used to generate in-plane excitation to the structure with a prescribed displacement record [35, 36]. In this study, the input is a scaled El Centro earthquake record with the maximum displacement of the shaker mass scaled to 1 inch. In order to calculate the exact shaker excitation force during the test, an accelerometer was installed on the moving mass of the shaker. The low-amplitude El Centro excitation caused little to no damage to the structure, thus the structure can be treated as a linear system in this study. To measure the dynamic response of the frame, a total of 44 acceleration channels (Kinemetrics EpiSensor ES-T [37] and ES-U [38]) were instrumented on the structure, including 27 in-plane longitudinal directions and 17 vertical directions. Specifically, the accelerometers were instrumented at mid-length and quarter length locations of columns and longitudinal beams. The sampling frequency is 200 Hz for all acceleration channels and the measured responses are filtered using an 8th order bandpass (0.5 ~ 50 Hz) Butterworth filter in both the forward and reverse directions to remove phase distortion.

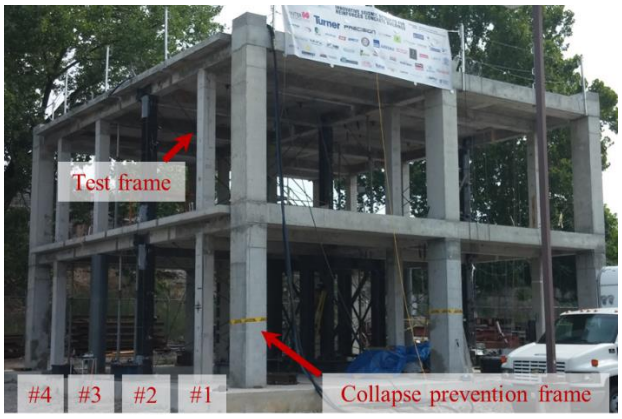

Figure 6 Full-scale test frame

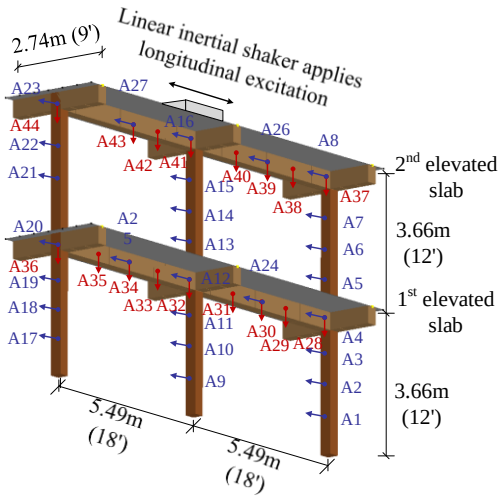

Figure 7 Accelerometer instrumentation

A finite element (FE) model of the concrete frame is built in SAP2000. The mesh size of the FE model is around 50.8 cm (20 in). The model contains a total of 2,482 degrees-of-freedom (DOFs). Because of the large size of the state-space system matrices (in Eq. (51) and (52)), model order reduction is needed. When n_{mode} of modes are used

for model order reduction, Ω denotes a diagonal matrix with diagonal entries as the first n_{mode} number of natural frequencies. In addition, denote the first n_{mode} number of the mass-normalized eigenvectors (vibrating mode shapes) as $\Psi = [\psi_1 \quad \psi_2 \quad \cdots \quad \psi_{n_{\text{mode}}}] \in \mathbb{R}^{n_{\text{DOF}} \times n_{\text{mode}}}$, where ψ_i is a column vector denoting the eigenvector of the i-th mode, i.e. $\psi_i = [\psi_{1,i} \quad \psi_{2,i} \quad \cdots \quad \psi_{n_{\text{DOF}},i}]^T$. The displacement vector q in physical coordinates is transformed to z in modal coordinates as $q = \Psi z$, where $z \in \mathbb{R}^{n_{\text{mode}}}$. Therefore, the reduced order model is given by Eq. (53) and (54).

$$\dot{x}_{mod} = \begin{Bmatrix} \dot{z} \\ \ddot{z} \end{Bmatrix} = \begin{bmatrix} 0 & \mathrm{I} \\ -\Omega^2 & -\Psi^T C_{\text{damp}} \Psi \end{bmatrix} \begin{Bmatrix} z \\ \dot{z} \end{Bmatrix} + \begin{bmatrix} 0 \\ \Psi^T \Gamma_u \end{bmatrix} u$$

$$\triangleq A_{c,mod} x_{mod} + B_{c,mod} u \tag{53}$$

$$y = \Gamma_y \ddot{q} + v = \Gamma_y \Psi \begin{bmatrix} -\Omega^2 & -\Psi^T C_{\text{damp}} \Psi \end{bmatrix} \begin{Bmatrix} z \\ \dot{z} \end{Bmatrix} + \Gamma_y \Psi \Psi^T \Gamma_u u + v$$

$$\triangleq C_{c,mod} x_{mod} + D_{c,mod} u + v \tag{54}$$

Because the first two in-plane modes contribute the most to the structural response under longitudinal shaking, n_{mode} is chosen as two. Detailed modal analysis from experimental measurements with comparison to the FE model is provided in [14] and summarized in Table 4. Based on the modal analysis result, the first two modes identified from experimental measurements can match well with the corresponding ones from the FE model. To obtain the continuous state space model, a Rayleigh damping model is used to construct the damping matrix C_{damp} based on the identified damping ratios of the first two modes. The natural frequency matrix Ω and the mode shape matrix Ψ are obtained from the FE model.

Table 4 Modal property comparison between FE model and experimental identification results

Mode	1st	2nd	3rd	4th
Experiment f_i^{EXP} (Hz)	2.00	5.41	13.92	19.82
FE model f_i^{FE} (Hz)	1.96	5.63	14.96	20.61
$\left(f_i^{\text{FE}} - f_i^{\text{EXP}}\right)/f_i^{\text{EXP}}$	-1.57%	4.16%	7.44%	4.00%
MAC values	0.999	0.988	0.935	0.887

5.1. Effect of sensor instrumentation on input estimation

For the reduced order model, the effect of sensor instrumentation on input estimation is discussed by examining the magnitude of the feedthrough matrix $D_{c,mod}$, which degenerates to a column vector in this single input example.

Because zero-order-hold discretization is used, the discrete feedthrough vector D of the estimators is the same as the continuous $D_{c,mod}$. Based on Eq. (54), a relatively large $D_{c,mod}$ is needed such that the unknown input u can be distinguished from measurement noise v. To derive an expression of the feedthrough vector of the reduced order model, denote the input DOF as the r-th DOF and the measured DOFs as the s_1, …, s_m-th DOFs of the full-order model. Therefore, the input location matrix $\Gamma_u \in \mathbb{R}^{n_{\mathrm{DOF}} \times n_u}$, which again degenerates to a column vector in this example, has value one at the r-th DOF and zero elsewhere. The output location matrix $\Gamma_y \in \mathbb{R}^{m \times n_{\mathrm{DOF}}}$ has value one at the j-th row and the s_j-th column with $j = 1, \ldots, m$; all other entries of Γ_y are zero. The $m \times 1$ feedthrough vector of the reduced order model can thus be expanded as follows.

$$\begin{aligned} D = D_{c,mod} &= \Gamma_y \Psi \Psi^T \{\Gamma_u\} = \Gamma_y \sum_{i=1}^{n_{\mathrm{mode}}} \begin{bmatrix} \psi_{1,i}^2 & \psi_{1,i}\psi_{2,i} & \cdots & \psi_{1,i}\psi_{n_{\mathrm{DOF}},i} \\ \psi_{2,i}\psi_{1,i} & \psi_{2,i}^2 & \cdots & \psi_{2,i}\psi_{n_{\mathrm{DOF}},i} \\ \vdots & \vdots & \ddots & \vdots \\ \psi_{n_{\mathrm{DOF}},i}\psi_{1,i} & \psi_{n_{\mathrm{DOF}},i}\psi_{2,i} & \cdots & \psi_{n_{\mathrm{DOF}},i}^2 \end{bmatrix} \{\Gamma_u\} \\ &= \sum_{i=1}^{n_{\mathrm{mode}}} \begin{Bmatrix} \psi_{s_1,i}\psi_{r,i} \\ \psi_{s_2,i}\psi_{r,i} \\ \vdots \\ \psi_{s_m,i}\psi_{r,i} \end{Bmatrix} \end{aligned} \tag{55}$$

Equation (55) shows that the magnitude of feedthrough vector $D_{c,mod}$ is determined by the product of eigenvector entries between the input DOF and the measured DOFs summed over each mode. For the j-th measurement, the product of $\psi_{s_j,i}$ and $\psi_{r,i}$ summed over n_{mode} modes needs to be large enough to ensure a relatively large value on the j-th row of $D_{c,mod}$. In this structural example, a total of 44 acceleration measurements are available, i.e. $m = 44$, including 27 longitudinal measurements and 17 vertical measurements. Figure 8 shows the entries of $\{D_{c,mod}\}_j$ with $j = 1, \ldots, 44$. Each entry corresponds to an acceleration measurement A_j as numbered in Figure 7. The larger values of $D_{c,mod}$ are from the longitudinal measurements located above the first elevated slab, i.e. A5~A8, A13~A16, A21~A23, A26 and A27. On the other hand, the entries of $D_{c,mod}$ corresponding to longitudinal measurements on and below the first elevated slab and all the vertical measurements are relatively small; these measurements contribute less to estimation of the longitudinal shaker input on the 2nd elevated slab.

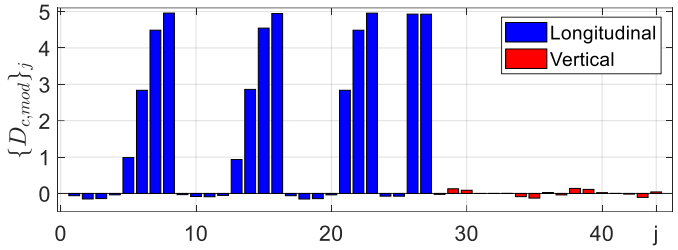

Figure 8 Entries of feedthrough vector $\{D_{c,mod}\}_j$, $j = 1, \dots, 44$. Each entry corresponds to acceleration measurement A_j.

5.2. Effect of covariance knowledge on input estimation

Before applying the estimators using field measurements, the effect of covariance parameters available to the estimators on input estimation is investigated in simulation first. In addition to the previously discussed three estimators, an online drift filter is combined with the WLS estimator to reduce drift error, denoted here as the WLSF estimator [14]. The online input drift filter is executed in real time, after each input estimation and before the state estimation. As a result, drift error in both input and state estimation can be reduced. The online drift filter used here is a 4th order high-pass Chebyshev Type I filter with cut-off frequency of 10^{-4} Hz and peak-to-peak passband ripple of 0.05 dB. Following the notations in Section 4.1, the covariances for the estimator operation include $\Sigma_{u,est}$ of the FIC estimator, $\Sigma_{\xi,est}$ of the AKF, and $\Sigma_{w,est}$ for all four estimators. Measurement noise covariance $\Sigma_{v,est}$ can be approximated based on sensor specification. The measured shaker excitation force is used as the input to simulate acceleration response of the structure. The standard deviation of measurement noise is set as $\sigma_v = 50$ μg, as obtained from a sensor noise level test. Accordingly, all estimators assume the same standard deviation of measurement noise of 50 μg. Note that this noise level corresponds to 1% to 20% of the intensity of the acceleration measurements obtained from the experiment, depending on the sensor location. The initial value of state estimation μ_{x_0} is set as 0 and the diagonal entries of Σ_{x_0} are set as 10^{-10} for all estimators to account for uncertainty in the initial condition of the structure. For AKF, $\hat{u}_0$, Σ_{u_0} and $\Sigma_{x_0 u_0}$ are set as zero. In this example, process noise w_k is only considered during estimation not in simulation, i.e. $\Sigma_{w,sim} = 0$.

To study the effect of estimator covariances on input estimation, the averaged input RMS error $\bar{e}_u$ is obtained from 20 trials in the same way described in Section 4.1. A same value of process noise covariance $\Sigma_{w,est}$ is used by all four estimators when performing estimation in 20 trials. The simulation of each trial lasts 30 seconds with

randomly generated white Gaussian measurements noise. In each trial, the WLS and the WLSF estimators are operated only once. On the other hand, the FIC estimator and AKF are performed for different values of $\Sigma_{u,est}$ and $\Sigma_{\xi,est}$ ranging from 0.5 to 10^7 kN^2. At each value of $\Sigma_{u,est}$ and $\Sigma_{\xi,est}$, input RMS error e_u is calculated accordingly. Among 20 trials, the averaged $\bar{e}_u$ of the FIC estimator and AKF can be obtained. When no process noise is applied, Figure 9(a) shows the relationship between $\bar{e}_u$ and the covariances of FIC and AKF in comparison to the results from the WLS and WLSF estimators. The smallest RMS error is 0.12 kN achieved by the FIC estimator when $\Sigma_{u,est}$ is around 5 kN^2. This is on the same order of magnitude to the calculated variance 1.7 kN^2 of the actual input signal during 1s ~ 6s, when the large excitation happens. For AKF, the estimator is not sensitive to the change of $\Sigma_{\xi,est}$, and the RMS error $\bar{e}_u$ is close to 0.64 kN, similar as the result from the WLS estimator; the two curves coincide in Figure 9(a). After combining the drift filter in WLS estimation, the RMS error is significantly reduced to 0.16 kN.

Figure 9(b) shows the result when a small amount of process noise is assumed for all the estimators by setting the covariance $\Sigma_{w,est}$ to be a diagonal matrix as $\Sigma_{w,est} = 10^{-12}I$. It can be observed that a small amount of process noise assumed by the estimators does not affect the RMS error significantly. In addition, the FIC estimator still performs better when $\Sigma_{u,est}$ is chosen between 0.5 and 30 kN^2. Furthermore, when $\Sigma_{u,est}$ becomes larger than 10^5, the results from FIC estimator converge to those of the WLS estimator in both cases.

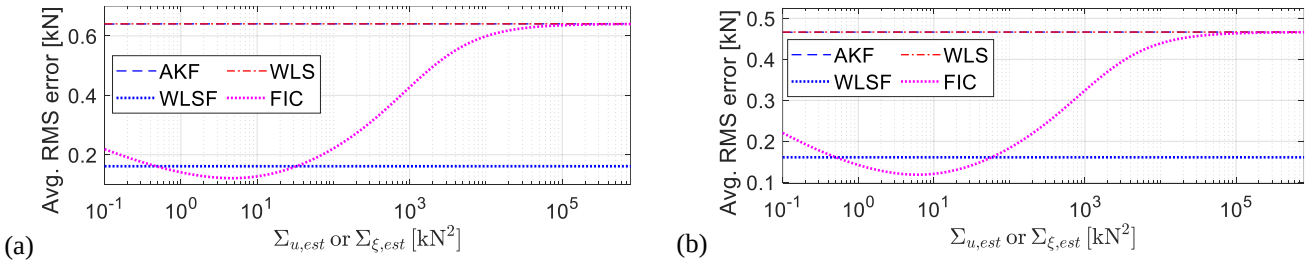

Figure 9 Averaged RMS error $\bar{e}_u$ of shaker input estimation: (a) $\Sigma_{w,sim} = \Sigma_{w,est} = 0$ (results from AKF and WLS coincide); (b) $\Sigma_{w,sim} = 0, \Sigma_{w,est} = 10^{-12}I$ (results from AKF and WLS coincide)

5.3. Input estimation with simulated acceleration responses

This subsection provides a single run of simulation to compare the estimated inputs from all four estimators. Because the dynamical state space system is accurate and no modeling error is assumed in simulation, process noise

covariance $\Sigma_{w,est}$ is set as 0. For the FIC estimator, $\Sigma_{u,est}$ is set as 5 kN^2. For AKF, because $\bar{e}_u$ is not sensitive to the value of $\Sigma_{\xi,est}$ as shown in Section 5.2, $\Sigma_{\xi,est}$ is set as the same as $\Sigma_{u,est}$ in this example. The measurement noise covariance and initial state covariance are set the same as those in Section 5.2. With a single trial of simulated acceleration response, Figure 10(a) shows the comparison of estimated inputs from 0s to 30s; Figure 10(b) shows the close-up plot of all four estimators during the initial 2s to 4s; Figure 10(c) ~ (f) shows the estimated input by of AKF, WLS, WLSF and FIC during the final 24s to 29s, respectively. The confidence interval of three times square root of input estimation error covariance, $\pm 3\sigma_{u_{k|k}}$, is included for the estimated input $\hat{u}_{k|k}$ obtained from each estimator. As shown in Figure 10(b), during the initial 2s ~ 4s, all estimators perform similarly well in estimating the shaker input. However, because of the drift error, both AKF (Figure 10(c)) and WLS (Figure 10(d)) could not estimate the input very well as simulation time increases. Figure 10(e) shows that although the online drift filter of WLSF estimator could reduce drift error from the WLS estimator, the input estimation error covariance still increases over time. In contrast, Figure 10(f) shows that the FIC estimator is able to estimate the input consistently well with a tight estimation confidence interval.

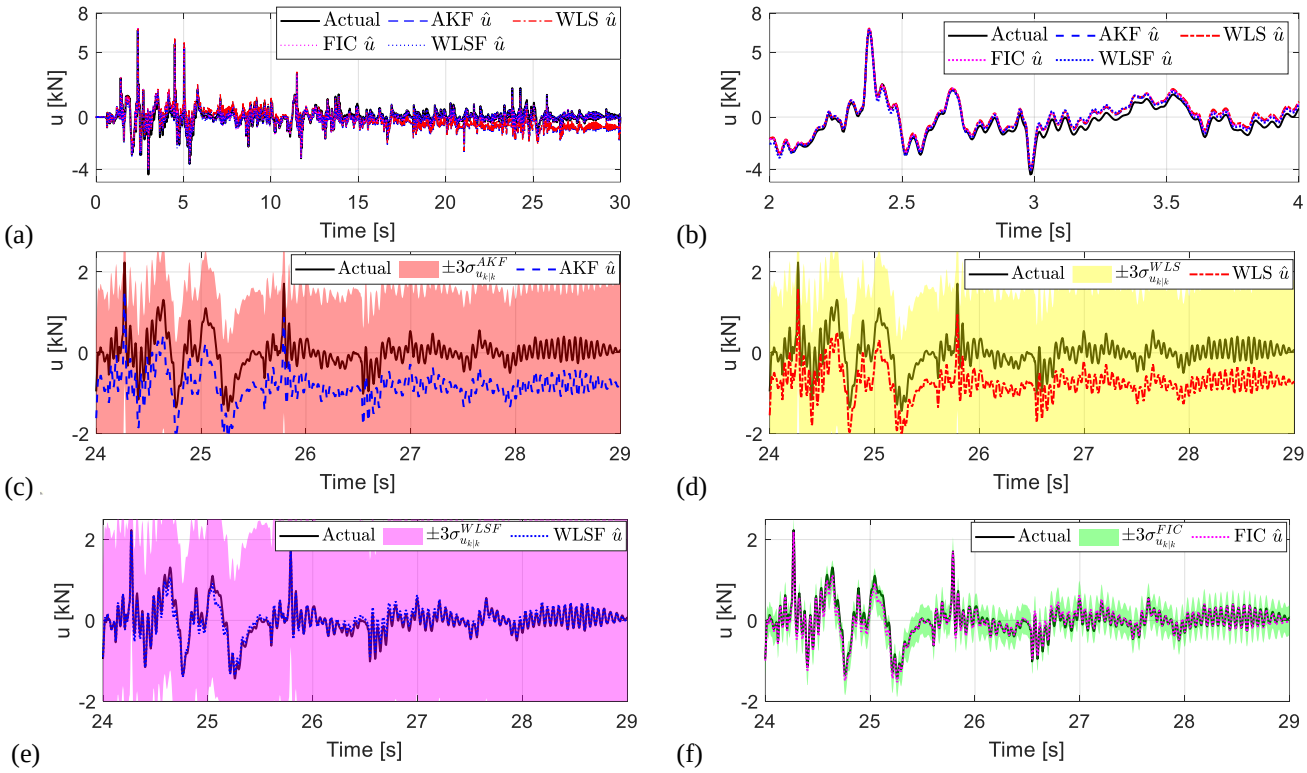

Figure 10 Estimation of shaker input with simulated measurements. (a) AKF, WLS, FIC and WLSF in 0~30s; (b) AKF, WLS, FIC and WLSF in 2~4s; (c) 24~29s of AKF estimation results; (d) 24~29s of WLS results; (e) 24~29s of WLSF results; (f) 24~29s of FIC results.

5.4. Input estimation with experimental acceleration measurements

The performance of AKF, WLS, FIC and WLSF estimators are further compared using experimental acceleration measurements. To account for potential modeling error when using experimental acceleration measurements, a non-zero process noise covariance $\Sigma_{w,est}$ is used by the estimators. The values of $\Sigma_{w,est}$ is determined based on the state estimation error covariance Σ_x during steady state, which is first obtained by setting $\Sigma_{w,est} = 0$. The process noise covariance $\Sigma_{w,est}$ is then set to be at least 100 times smaller than the corresponding states error covariance. As a result, the four diagonal entries of $\Sigma_{w,est}$ are chosen as 10^{-10},10^{-12}, 10^{-10} and 10^{-12}, respectively. The other estimator covariance parameters, i.e. $\Sigma_{u,est}$ of FIC, $\Sigma_{\xi,est}$ of AKF and measurement noise covariance Σ_v are the same as those used in Section 5.3.

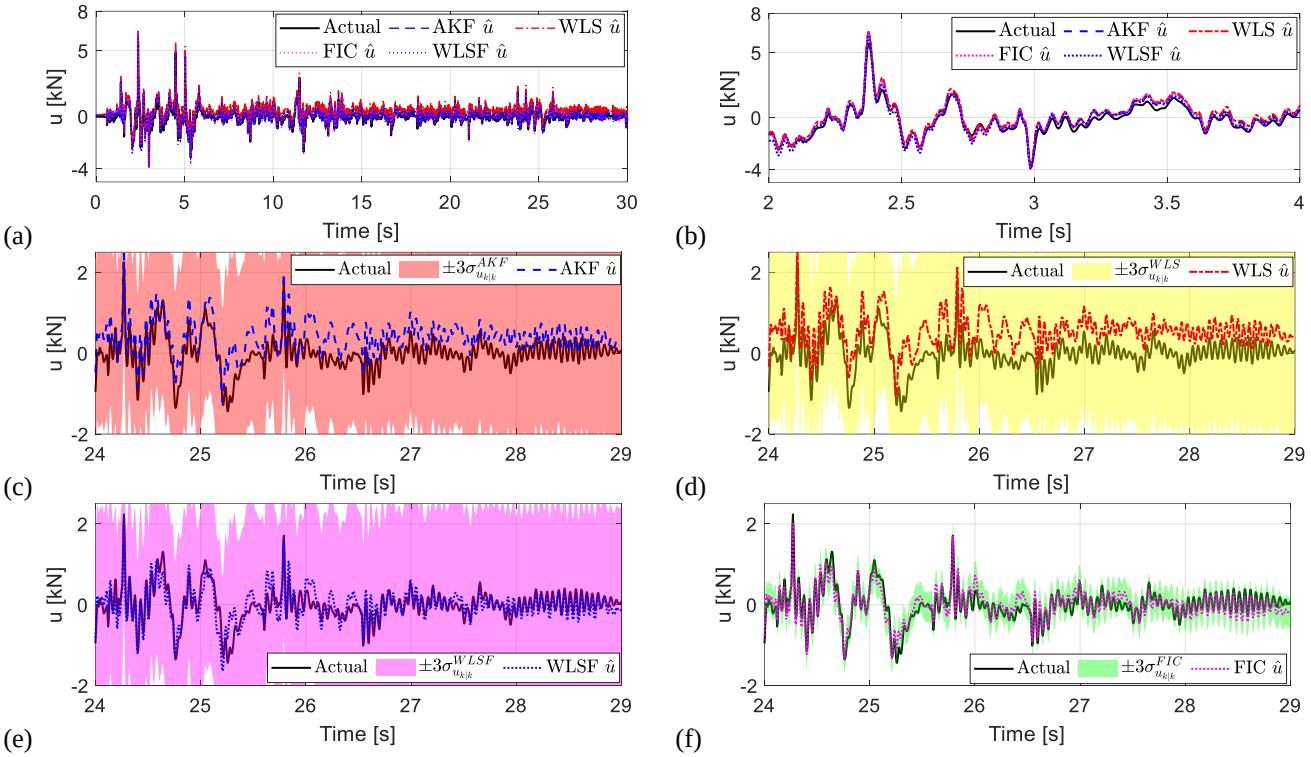

Figure 11 Estimation of shaker input with experimental measurements. (a) AKF, WLS, FIC and WLSF in 0~30s; (b) AKF, WLS, FIC and WLSF in 2~4s; (c) 24~29s of AKF estimation results; (d) 24~29s of WLS results; (e) 24~29s of WLSF results; (f) 24~29s of FIC results.

Figure 11(a) shows the comparison of estimated inputs from 0s to 30s; Figure 11(b) shows the close-up plots of the initial 2s to 4s; Figure 11(c) ~ (f) shows the estimated input from AKF, WLS, WLSF and FIC estimator during the final 24s to 29s, respectively. All four estimators perform similarly at the beginning (Figure 11(b)) while drift error persists in AKF and WLS estimation as time increases. As shown in Figure 11(c) and (d), the AKF and WLS

estimator show a large drift error in the estimated input as well as a large estimation error covariance. As for WLSF, Figure 11(e) shows the online drift filter of the WLSF estimator can again improve the WLS performance by reducing drift error but could not decrease the estimation error covariance. In contrast, the FIC estimator can estimate the input well with a small error covariance (Figure 11(f)).

Because only FIC and WLSF can provide a good estimate of the input over time, the input estimation error covariance $\Sigma_{u_{k|k}}$ and state estimation error covariance $\Sigma_{x_{k|k}}$ of these two estimators are further discussed here. Figure 12(a) shows that for the FIC estimator, the input estimation error covariance $\Sigma_{u_{k|k}}$ converge to steady state after around 8s. In contrast, the input error covariance of WLSF cannot converge to steady state. Figure 12(b) shows the time history of state estimation error covariance $\Sigma_{x_{k|k}}$ of FIC and WLSF. For the FIC estimator, the error covariances of all states converge to steady state, but the error covariances of x_1 and x_2 from the WLSF cannot converge to steady state, even though the error covariances of x_3 and x_4 are able to converge. Same phenomenon can be observed for AKF and the WLS estimator without drift filter and is not further included here. It should be noted that a longer simulation time could not help the error covariance of AKF and WLS to converge. Instead, the error covariance keeps increasing over time. This again indicates the AKF and WLS estimator are not completely observable. Although an online drift filter is able to reduce drift error, it cannot resolve the un-observability issue.

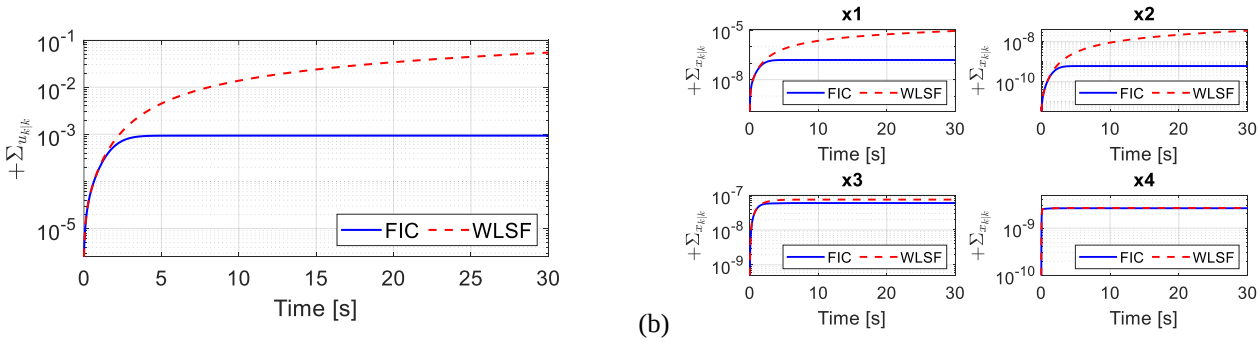

Figure 12 Convergence of estimation error covariance of FIC and WLSF: (a) input estimation error covariance $\Sigma_{u_{k|k}}$ of FIC and WLSF; (b) state estimation error covariance $\Sigma_{x_{k|k}}$ of FIC and WLSF (in modal coordinates)

In summary, in both simulation and experimental validation, both the FIC and WLSF estimator result in smaller input estimation error compared to AKF and WLS estimator. Furthermore, although the WLSF perform similar well as the FIC estimator when experimental measurements are used, the online drift filter requires pre-tuning of the filter order, cutoff frequency and passband ripple. In contrast, the input covariance $\Sigma_{u,est}$ of the FIC estimator can be set

based on any available statistical property of the input signal. For example, if the covariance of the unknown input can be obtained as prior knowledge for the type of input expected in certain application, $\Sigma_{u,est}$ should be simply set the same as the covariance. If the covariance cannot be determined a priori, the expected input magnitude can be used to approximate the input covariance and set as $\Sigma_{u,est}$ by the estimator. Specifically, for the El Centro input in this example, the best choice of $\Sigma_{u,est}$ is around 5 kN^2 (Section 5.2); the resulting standard deviation $\sigma_{u,est} = 2.24$ kN is around the same order of magnitude as the input (Figure 10 (a)). In addition, the FIC estimator can provide a tighter estimation confidence interval and the estimator can converge to steady state (Figure 12). It should also be noted that when using experimental data, modeling error can be seen affecting all estimator performance caused by the discrepancy between the FE model and the actual structure. Future FE model updating can be used to further improve the estimation results.

6. Conclusion

This paper presents a unifying MMSE framework for simultaneous input-state estimation for systems with direct feedthrough of the unknown input when the exact state space model of the input is not available. The finite input covariance (FIC) estimator is proposed when assuming the unknown input is white Gaussian with covariance Σ_u. Proof is provided that when the input covariance of the white Gaussian input approaches infinity, the FIC estimator is theoretically equivalent to the weighted least squares (WLS) estimator proposed by Gillijns *et al*. in [6]. Such flexibility of the FIC estimator helps to utilize any available property of the unknown input, such as the standard deviation or maximum magnitude. When no information of the input is available, the FIC estimator can be readily converted to the WLS estimator. In addition, when a finite input covariance is used, drift error can be eliminated, and a tighter estimation confidence interval can be achieved by the FIC estimator when only acceleration measurements are available. The FIC estimator is validated and compared with an augmented Kalman filter (AKF) assuming a Gaussian random walk input model and the WLS estimator using data from both simulation and field test. The equivalence between the FIC estimator and the WLS estimator can be demonstrated when Σ_u is larger than a certain level. In addition, smaller error can be achieved by the FIC estimator when Σ_u is close to the actual statistical property of the unknown input.

While due to page limit the paper only described studies with one input channel, the proposed FIC estimator can provide similar performance for the identification of multiple inputs with MIMO systems. When estimating multiple inputs, it is also recommended to maintain the full-column rank of the feedthrough matrix D, and devise a measurement system that provides relatively large Du_k entries (in comparison to the measurement noise v_k). Finally, as an ongoing research topic, for systems without direct feedthrough of the unknown input, a similar framework can be used to derive the theoretical relationship among all the estimators.

7. Acknowledgements

This research was partially funded by the National Science Foundation (CMMI- 1634483). Any opinions, findings, and conclusions or recommendations expressed in this publication are those of the authors and do not necessarily reflect the view of the sponsors.

References

[1] P. K. Kitanidis, "Unbiased minimum-variance linear state estimation," *Automatica,* vol. 23, no. 6, pp. 775-778, 1987.
[2] Y. Bar-Shalom, X. R. Li, and T. Kirubarajan, *Estimation with applications to tracking and navigation: theory algorithms and software*. John Wiley & Sons, 2004.
[3] B. Friedland, "Treatment of bias in recursive filtering," *IEEE Transactions on Automatic Control*, vol. 14, no. 4, pp. 359-367, 1969.
[4] E. I. Verriest, "Optimal filtering for crypto-deterministic systems with application to delay systems with unknown initial data," *Proceedings of the 47th IEEE Conference on Decision and Control*, pp. 49-54: IEEE, 2008.
[5] M. Darouach, M. Zasadzinski, and M. Boutayeb, "Extension of minimum variance estimation for systems with unknown inputs," *Automatica,* vol. 39, no. 5, pp. 867-876, 2003.
[6] S. Gillijns and B. De Moor, "Unbiased minimum-variance input and state estimation for linear discrete-time systems with direct feedthrough," *Automatica,* vol. 43, no. 5, pp. 934-937, 2007.
[7] E. Lourens, C. Papadimitriou, S. Gillijns, E. Reynders, G. De Roeck, and G. Lombaert, "Joint input-response estimation for structural systems based on reduced-order models and vibration data from a limited number of sensors," *Mechanical Systems and Signal Processing,* vol. 29, pp. 310-327, 2012.
[8] K. Maes, A. Smyth, G. De Roeck, and G. Lombaert, "Joint input-state estimation in structural dynamics," *Mechanical Systems and Signal Processing,* vol. 70, pp. 445-466, 2016.
[9] K. Maes, K. V. Nimmen, E. Lourens, A. Rezayat, P. Guillaume, G. D. Roeck, and G. Lombaert, "Verification of joint input-state estimation for force identification by means of in situ measurements on a footbridge," *Mechanical Systems and Signal Processing,* vol. 75, pp. 245-260, 2016.
[10] E. Lourens, E. Reynders, G. De Roeck, G. Degrande, and G. Lombaert, "An augmented Kalman filter for force identification in structural dynamics," *Mechanical Systems and Signal Processing,* vol. 27, pp. 446-460, 2012.
[11] S. E. Azam, E. Chatzi, and C. Papadimitriou, "A dual Kalman filter approach for state estimation via output-only acceleration measurements," *Mechanical Systems and Signal Processing,* vol. 60, pp. 866-886, 2015.
[12] S. E. Azam, E. Chatzi, C. Papadimitriou, and A. Smyth, "Experimental validation of the Kalman-type filters for online and real-time state and input estimation," *Journal of vibration and control,* vol. 23, no. 15, pp. 2494-2519, 2017.

[13] F. Naets, J. Cuadrado, and W. Desmet, "Stable force identification in structural dynamics using Kalman filtering and dummy-measurements," *Mechanical Systems and Signal Processing,* vol. 50, pp. 235-248, 2015.
[14] X. Liu and Y. Wang, "Input estimation of a full-scale concrete frame structure with experimental measurements," *Proceedings of the 37th International Modal Analysis Conference (IMAC XXXVII),* Orlando, FL, USA, 2019.
[15] M. Valikhani and D. Younesian, "Bayesian framework for simultaneous input/state estimation in structural and mechanical systems," *Structural Control and Health Monitoring,* p. e2379, 2019.
[16] O. Sedehi, C. Papadimitriou, D. Teymouri, and L. S. Katafygiotis, "Sequential Bayesian estimation of state and input in dynamical systems using output-only measurements," *Mechanical Systems and Signal Processing,* vol. 131, pp. 659-688, 2019.
[17] R. Nayek, S. Chakraborty, and S. Narasimhan, "A Gaussian process latent force model for joint input-state estimation in linear structural systems," *Mechanical Systems and Signal Processing,* vol. 128, pp. 497-530, 2019.
[18] X. Liu, "Simultaneous input and state estimation through a unifying MMSE framework with applications in structural dynamics," Ph.D. Dissertation, Civil and Environmental Engineering, Georgia Institute of Technology, Atlanta,GA,USA, 2019.
[19] S. Sarkka, M. A. Alvarez, and N. D. Lawrence, "Gaussian process latent force models for learning and stochastic control of physical systems," *IEEE Transactions on Automatic Control,* 2018.
[20] W.-H. Chen, "Disturbance observer based control for nonlinear systems," *IEEE/ASME transactions on mechatronics,* vol. 9, no. 4, pp. 706-710, 2004.
[21] H. Sun, D. Feng, Y. Liu, and M. Q. Feng, "Statistical regularization for identification of structural parameters and external loadings using state space models," *Computer-Aided Civil and Infrastructure Engineering,* vol. 30, no. 11, pp. 843-858, 2015.
[22] H. Sun and O. Büyüköztürk, "Identification of traffic-induced nodal excitations of truss bridges through heterogeneous data fusion," *Smart Materials and Structures,* vol. 24, no. 7, p. 075032, 2015.
[23] F. Naets, J. Croes, and W. Desmet, "An online coupled state/input/parameter estimation approach for structural dynamics," *Computer Methods in Applied Mechanics and Engineering,* vol. 283, pp. 1167-1188, 2015.
[24] Y. Lei, D. Xia, K. Erazo, and S. Nagarajaiah, "A novel unscented Kalman filter for recursive state-input-system identification of nonlinear systems," *Mechanical Systems and Signal Processing,* vol. 127, pp. 120-135, 2019.
[25] R. Astroza, H. Ebrahimian, Y. Li, and J. P. Conte, "Bayesian nonlinear structural FE model and seismic input identification for damage assessment of civil structures," *Mechanical Systems and Signal Processing,* vol. 93, pp. 661-687, 2017.
[26] H. Ebrahimian, R. Astroza, J. P. Conte, and C. Papadimitriou, "Bayesian optimal estimation for output-only nonlinear system and damage identification of civil structures," *Structural Control and Health Monitoring,* vol. 25, no. 4, p. e2128, 2018.
[27] S. Pan, D. Xiao, S. Xing, S. Law, P. Du, and Y. Li, "A general extended Kalman filter for simultaneous estimation of system and unknown inputs," *Engineering Structures,* vol. 109, pp. 85-98, 2016.
[28] M. I. Friswell and J. E. Mottershead, *Finite element model updating in structural dynamics* (Solid mechanics and its applications ; v. 38). Dordrecht; Boston: Kluwer Academic Publishers, 1995, pp. xii, 286 p.
[29] B. Jaishi and W. X. Ren, "Damage detection by finite element model updating using modal flexibility residual," *Journal of Sound and Vibration,* vol. 290, no. 1-2, pp. 369-387, Feb 2006.
[30] C. Farhat and F. M. Hemez, "Updating finite element dynamic models using an element-by-element sensitivity methodology," *AIAA Journal,* vol. 31, no. 9, pp. 1702-1711, 1993.
[31] J. E. Mottershead, M. Link, and M. I. Friswell, "The sensitivity method in finite element model updating: a tutorial," *Mechanical Systems and Signal Processing,* vol. 25, no. 7, pp. 2275-2296, 2011.
[32] D. Zhu, X. Dong, and Y. Wang, "Substructure stiffness and mass updating through minimization of modal dynamic residuals," *Journal of Engineering Mechanics,* vol. 142, no. 5, p. 04016013, 2016.
[33] G. James, T. G. Carne, and J. P. Lauffer, "The natural excitation technique (NExT) for modal parameter extraction from operating structures," *Modal Analysis-the International Journal of Analytical and Experimental Modal Analysis,* vol. 10, no. 4, p. 260, 1995.

[34] J. Ching and J. Beck, "Real-time reliability estimation for serviceability limit states in structures with uncertain dynamic excitation and incomplete output data," *Probabilistic engineering mechanics,* vol. 22, no. 1, pp. 50-62, 2007.
[35] E. Yu, D. H. Whang, J. P. Conte, J. P. Stewart, and J. W. Wallace, "Forced vibration testing of buildings using the linear shaker seismic simulation (LSSS) testing method," *Earthquake engineering & structural dynamics,* vol. 34, no. 7, pp. 737-761, 2005.
[36] X. Dong, X. Liu, T. Wright, Y. Wang, and R. DesRoches, "Validation of wireless sensing technology densely instrumented on a full-scale concrete frame structure," *Proceedings of International Conference on Smart Infrastructure and Construction (ICSIC)*, Cambridge, U.K., June 27-29, 2016.
[37] Kinemetrics, "EpiSensor (ES-T) Datasheet," ed. www.kinemetrics.com, 2018.
[38] Kinemetrics, "EpiSensor (ES-U2) Datasheet," ed. www.kinemetrics.com, 2018.